NWC TP 4702
Part 1
COPY 25

EXPLOSIVELY DISPERSED LIQUIDS

Part 1. DISPERSION MODEL

by

Richard J. Zabelka
Lloyd H. Smith
Propulsion Development Department

ABSTRACT. A preliminary analysis of the dispersion process of liquid droplets into an aerosol cloud is presented. This assessment of the complex phenomena is not all encompassing, but is believed to shed some light upon the behavior of the various mechanisms which govern the expansion of explosively dispersed liquids. This analysis does provide a basic understanding, and provides data for preliminary design estimates.

The equations presented are based on the concept of a fluid piston in the first three of four regimes of motion. This fluid piston is essentially a gas bubble surrounded by a liquid shell. As the gas bubble expands it forces the liquid outward to form the characteristic explosive dispersion cloud. The fluid piston degenerates into discrete droplets, whose motion is governed by aerodynamic forces in Regime IV.

These equations of motion were developed from experimental data collected with two different size devices. The agreement with this data indicates that scaling requirements are satisfied.

NAVAL WEAPONS CENTER
CHINA LAKE, CALIFORNIA * DECEMBER 1969

NAVAL WEAPONS CENTER
AN ACTIVITY OF THE NAVAL MATERIAL COMMAND

M. R. Etheridge, Capt., USN ..... Commander
Thomas S. Amlie, Ph.D. ..... Technical Director

FOREWORD

This investigation was conducted during the period May 1967 until December 1968 in direct support of development programs. This effort was funded under AirTask A35-532-050/216-1/W11-62X and additional funding was provided under Marine Corps Commitment Authorization WR-27-8-7721.

This report summarizes the first part of a proposed two part effort to develop a understanding of the mechanics of explosive dispersion of liquids. The Part 1 effort consists of a dispersion model, describing the mechanisms by which the liquid is explosively forced into an expanding cloud.

Released by
P. E. CORDLE, Head
Warhead Division
1 December 1969

Under authority of
G. W. LEONARD, Head
Propulsion Development Department

NWC Technical Publication 4702, Part 1

Published by ..... Propulsion Development Department
Collation ..... Cover, 35 leaves, DD Form 1473, abstract cards
First printing ..... 100 numbered copies
Security classification ..... UNCLASSIFIED

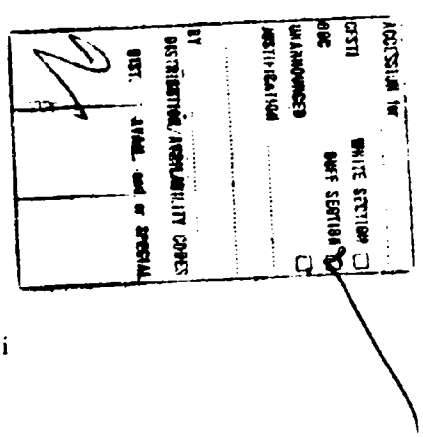

CONTENTS

INTRODUCTION

The dispersion of an aerosol cloud of liquid droplets by means of the detonation of an explosive charge within a canister of liquid is becoming of increasing interest for military purposes. Furthermore, the process may have potential civilian applications for the dispersion of liquids (or even solid powders) for such purposes as firefighting or fertilizing crops, in which chemicals might be dispersed rapidly over large areas.

In order to properly employ explosive dispersion techniques with maximum effectiveness, we must better understand the complex physical phenomena making up the explosive dispersion process. In particular, we have to understand those factors controlling the expansion of the cloud in the atmosphere so that the devices can be designed to disperse the material into the desired cloud configuration with the desired concentration.

In this report we have attempted a preliminary analysis of the dispersion process based on the experimental information which is available and which can be published in an unclassified report. We don't in any sense represent this as "the" analysis of the cloud dispersion process, but do believe it will shed some light on the complex physical phenomena which govern the expansion of explosively dispersed clouds and enable us to at least begin to predict the behavior of these clouds. Considerably more experimental and analytical work will be required before we can claim fully to understand the process.

BACKGROUND

A typical device for the explosive dispersion of a liquid is illustrated in Fig. 1. It consists of a metal canister into which the ends are welded. Usually the canister is scored with longitudinal grooves placed approximately 15 degrees apart to insure that breakup of the canister is uniform. A metal tube which contains the explosive burster charge is located along the axis of the canister and is constructed so that the explosive charge may be inserted after the canister is filled with liquids and sealed. A detonator is placed in close proximity to the explosive charge as shown. Table 1 lists the dimensions and capacities of two typical devices, one containing three pounds of liquid and the other 83 pounds.

Upon the detonation of the burster explosive the liquid is forced outward with such energy that it breaks up into aerosol droplets which disperse in a few milliseconds to form a toroid-shaped cloud as shown in Fig. 2. The concentration of liquid droplets is much less near the

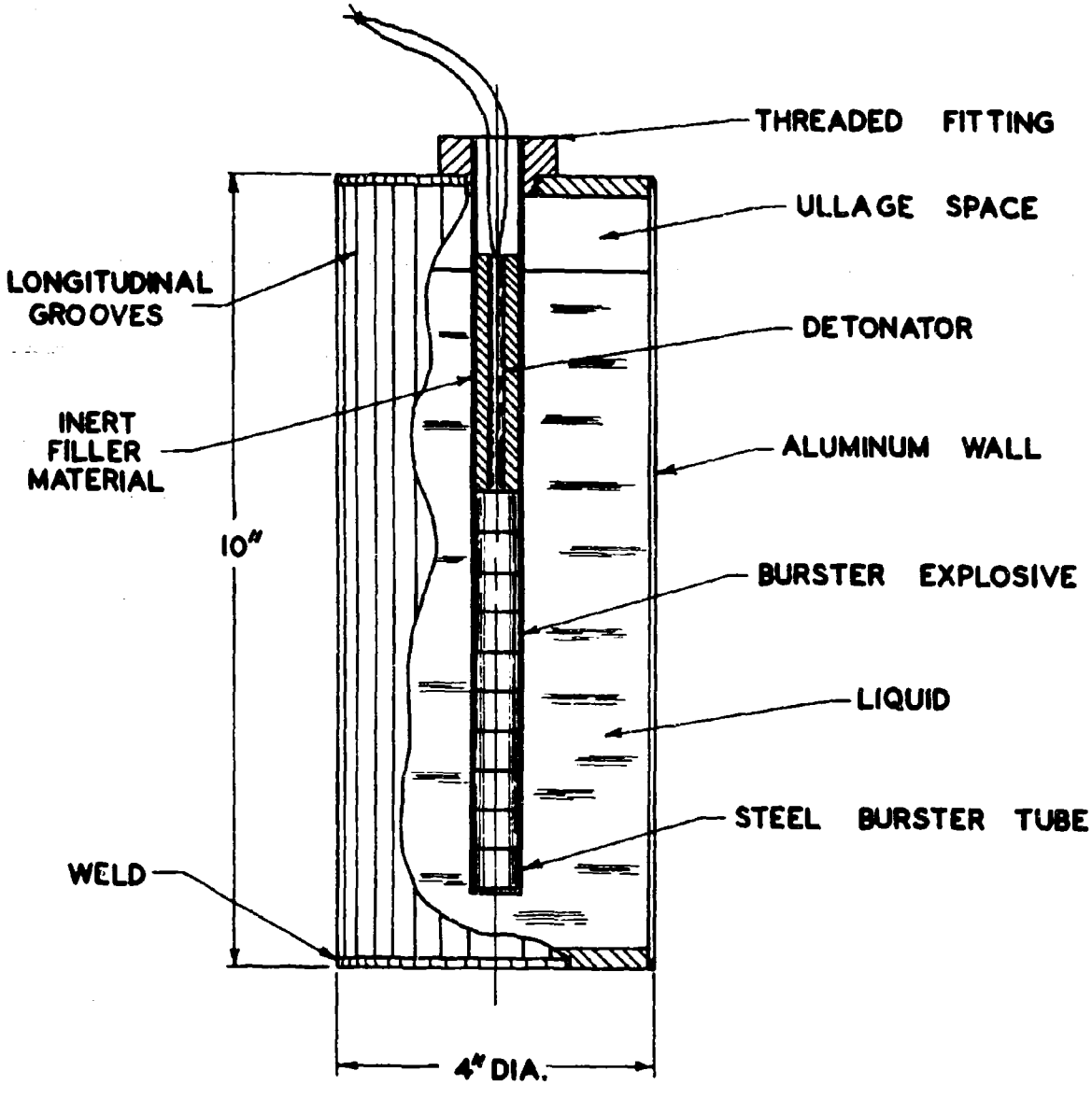

FIG. 1. Typical Three-Pound Explosive Dispersion Device.

TABLE 1. Dimensions and Capacities of Explosive Dispersion Devices.

	Three-pound	Eighty-three pound
Liquid weight	3 lb	83 lb
Liquid density (typical)	1.80 slug/ft^3	1.80 slug/ft^3
Liquid volume	5.18×10^{-2} ft^3	1.43 ft^3
Explosive weight	0.053 lb	0.728 lb
Explosive density	3.10 slug/ft^3	3.10 slug/ft^3
Explosive volume	5.70×10^{-4} ft^3	7.29×10^{-3} ft^3
Canister length	0.833 ft	1.60 ft
Canister diameter	0.333 ft	1.12 ft
Canister wall thickness	0.065 in	0.062 in
Canister material	Alum. (6061 T-4)	Steel (1020)
Burster tube volume	11.4×10^{-4} ft^3	8.11×10^{-3} ft^3
Burster tube diameter	0.625 in	1.065 in
Burster tube wall thickness	0.035 in	0.035 in
Burster tube material	Steel (4130)	Steel (4130)
End plate thickness	0.25 in	0.375 in

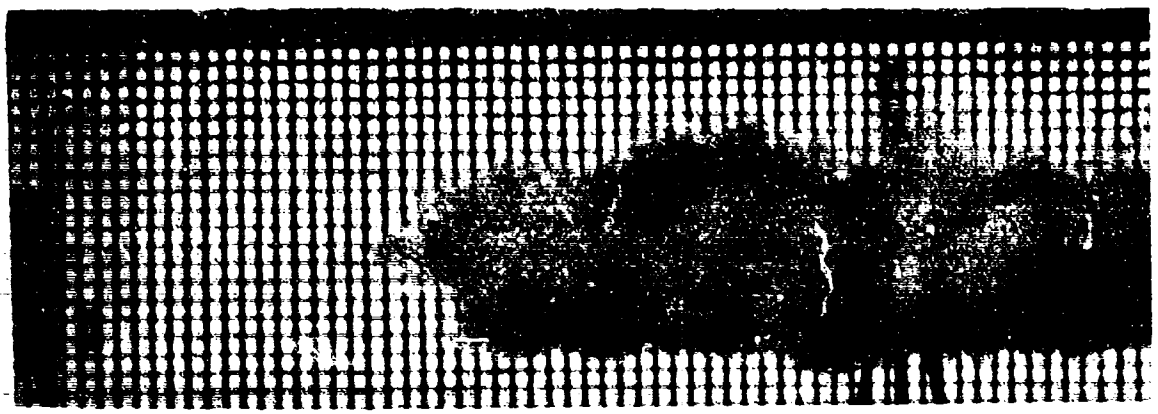

Side View

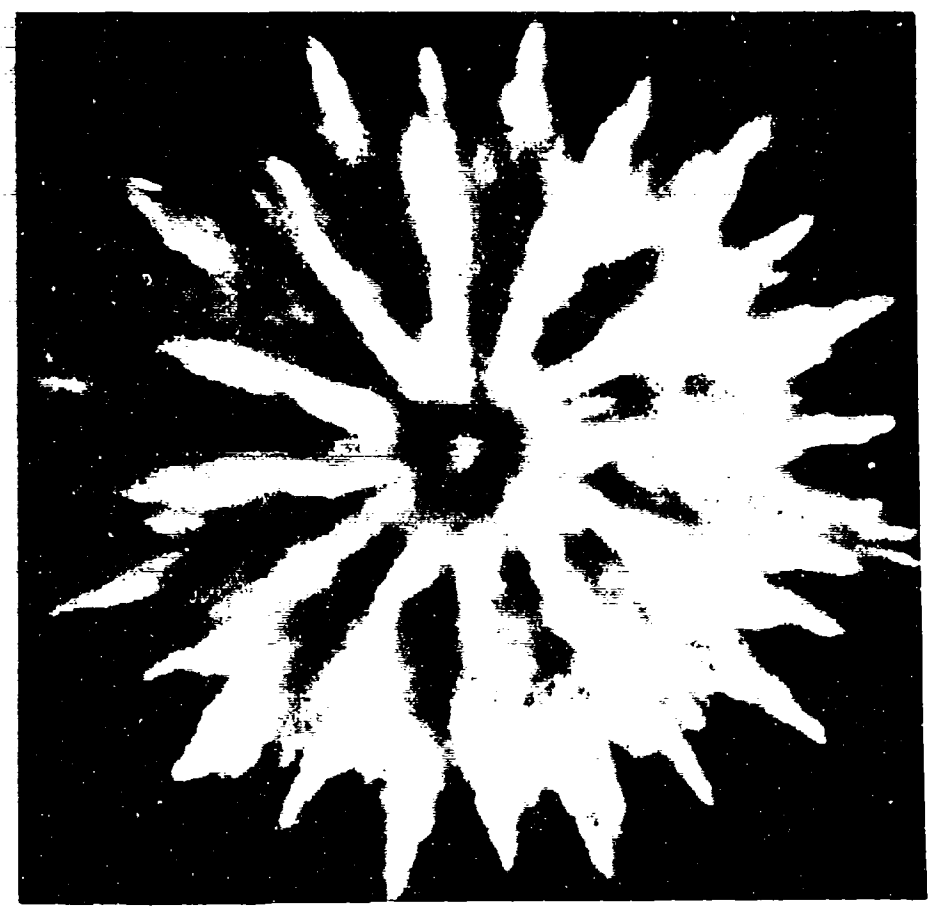

Overhead View

FIG. 2. Typical Cloud.

center of the cloud than in the portion near the outer edge. The shape of the cloud is complex in that "spikes" of liquid are forced outward from the main body of the cloud as the expansion proceeds.

In previous investigations it has been assumed that the cloud is a toroidal mass in which the radial velocity is constant with respect to circumferential position. Attempts were made to plot the edge of the cloud as it expanded radially and it was implicitly assumed that the edge of the cloud, as seen from the side, was composed of the same droplets throughout the expansion process. Robbins, for example, in Ref. 1 and 2 photographed the outward expansion of the cloud and obtained a composite radius versus time plot for representative devices. The present authors, along with Douglas Kinney, used the same technique in an early report and then attempted to derive an empirical relation for the equation of motion based on the Gurney formula for the expansion of explosive products (Ref. 3).

It soon became apparent in the present study, however, that such an approach was not going to yield meaningful results in terms of understanding the physical phenomena which were controlling the expansion of the droplets of liquid. The cloud does not expand uniformly with respect to circumferential position. It is well known that spikes of liquid follow the fragments or strips of canister material as they travel outward. Those "strip spikes" travel outward considerably further than the main body of the cloud. Furthermore, another type of spike, which we call a "squirt spike", occurs at the time of canister rupture. The squirt spikes are caused by liquid squirting outward through the cracks in the canister as it ruptures along the longitudinal grooves. The squirt spikes initially travel some 200 ft/sec faster than the cloud body, but slow down more quickly.

An observer viewing the cloud from the side will see first the squirt spikes leading the remainder of the cloud. Later the cloud body will pass the squirt spikes and finally the droplets composing the strip spikes will move out in front. Thus, the expansion sequence is complex in that different physical processes govern the expansion of different portions of the cloud. It certainly may be possible to develop a single empirical equation which can be used to describe the position of the cloud at any time, but such an equation would not assist us in understanding the physics of the dispersion process. To do this we must treat each portion of the cloud separately and attempt to develop equations of motion which described the physical processes which are occurring in the cloud.

EXPERIMENTAL DATA

Only a limited amount of detailed experimental data of a quantitative nature is available, and most of this is for the experimental three-pound device. We have, therefore, based this study primarily on the

information available for the three-pound device. We have also attempted to scale up the analysis to match information which is available for a device containing 83 pounds of liquid.

Inspection of photographs taken at approximately 6000 frames per second by means of a Fastax camera showed that during the dispersion of a cloud from a three-pound canister a shock wave breaks away from the canister at about the time the walls begin to move outward. This shock wave has been observed by other experimenters. It is assumed that the shock wave is the result of the detonation wave from the burster charge propagating outward through the liquid and the canister walls and into the atmosphere. The shock wave is quite weak and has an initial speed[1] of only 200 or 300 ft/sec greater than the speed of the canister walls as they expand. Thus the majority of the energy of the detonation wave has been given up to the liquid and the canister walls before the wave emerges.

Examination of photos of the same devices taken with a Cordin camera at framing rates of approximately 125,000 frames per second indicates that the canister expands before breaking. The time from first motion of the canister until rupture is about 0.0004 seconds. The canister begins to break near the center of the longitudinal grooves and liquid immediately begins to squirt out through the resulting orifices which are formed. This phenomenon can be seen in Fig. 3, which is a reproduction of a typical Cordin camera framing sequence. The liquid which squirts outward from the canister as it is breaking into strips is that which forms the squirt spikes.

As the canister expands further it breaks into discrete fragments or strips which fly outward. The lid and the bottom of the canister are also separated and fly up and down respectively, although at lower speeds.

The main body of the cloud can begin to expand into the atmosphere only after the canister has broken. Since the fragments are initially behind the squirt spikes, and are traveling more slowly, they initially are not visible in photographs taken of the side of the cloud. The forward edge of the cloud is the forward edge of the squirt spikes for the first few milliseconds. Figure 4 is taken from overhead photographs of a typical three-pound device during dispersion and illustrates the expansion pattern of the spikes and main body of the cloud. The framing rate was approximately 3400 frames per second.

The fragments do not decelerate as rapidly as the droplets comprising the squirt spikes and, as the cloud expands, the fragments catch up with and pass the squirt spikes. Because the fragments create

[1]Speed is used throughout, as opposed to velocity, since the direction is only assumed to be radial and speed represents the gross magnitude of all the particles collectively.

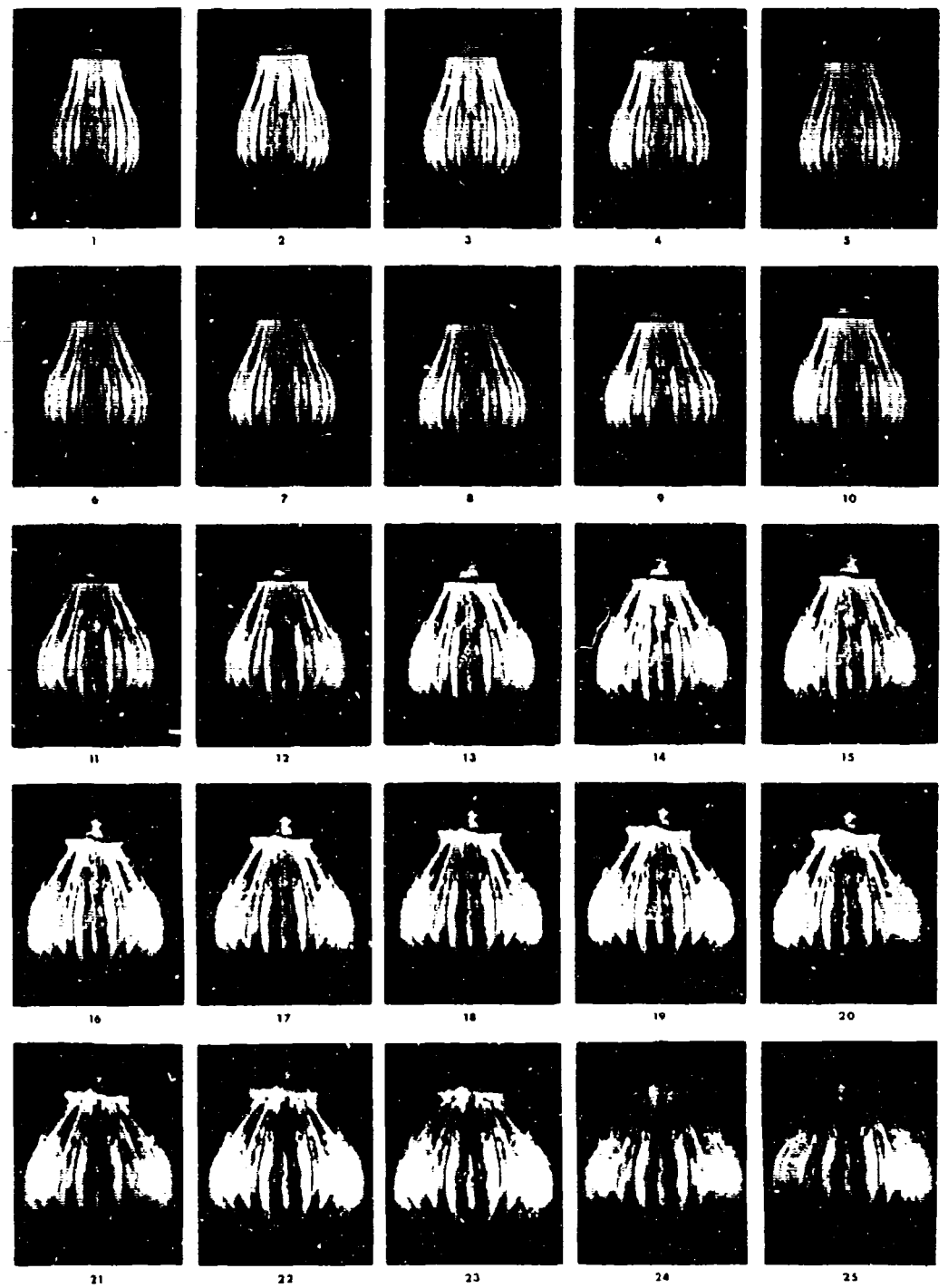

FIG. 3. Canister Rupture.

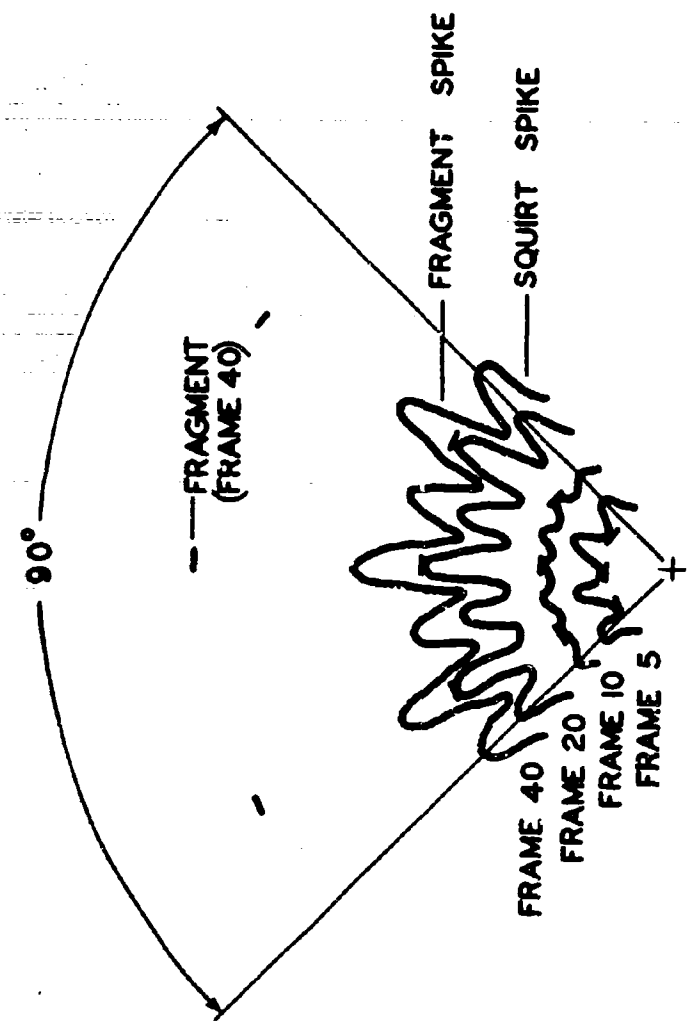

FIG. 4. Expansion of Spikes.

wakes behind them they drag a certain portion of the liquid droplets behind them as they fly outward. Those droplets form the strip or fragment spikes, and those droplets pass the squirt spikes and become the leading edge of the cloud as it expands.

The droplets comprising the main body of the cloud expand at a slower rate than the droplets in either of the spikes. We estimate, however, that the droplets in the main body comprise more than 90% of the total mass of the cloud. Hence it is the rate and distance of expansion of the main body droplets, not the spikes, which is important. Fortunately the spikes are thin and tenuous and in the side view the main body of the cloud can usually be differentiated from the spikes. Thus, the information on the expansion rate and distance of the main body of the cloud usually can be obtained from a careful assessment of the experimental data. The main body of the cloud never expands to the extent that the fragment spikes do, but we consider that the actual useful diameter of the cloud is that of the main body, and not that of the spikes.

SHOCK WAVE PROPAGATION DISTANCE AND RATE

The shock wave from a three-pound device was photographed using Fastax cameras at framing rates of approximately 6000 frames per second. Figure 5 illustrates the shock wave radius as a function of time for a typical three-pound device. The initial shock wave speed appears to be about 1500 ft/sec as recorded by both cameras. The shock decays slowly, but must eventually reach a minimum speed of approximately 1140 ft/sec, the speed of sound in air. It was impossible to read the shock wave position beyond approximately 10 milliseconds because it became too weak to be visible against the backdrop.

The only quantitative shock speed information we have available is that for the three-pound device. The information gained from different experimental firings agrees quite well. It has not been feasible to attempt to obtain shock speed information for larger devices since the detonation of the larger bursters would damage the experimental gridded backdrop which is used to read the shock position.

FRAGMENT RADIUS AND SPEED

The intial radius versus time relation of the fragments could be obtained from the Cordin camera photographs for two typical firings as shown in Fig. 6. Because of the difficulty of synchronising the cameras with the detonations, the two sets of data are displaced from each other by a tenth of a millisecond. Nevertheless the slopes of the curves are approximately the same and indicate initial fragment speeds of approximately 1100 ft/sec. The initial speed of the fragments is also the initial speed of the main body of the cloud since the liquid (other

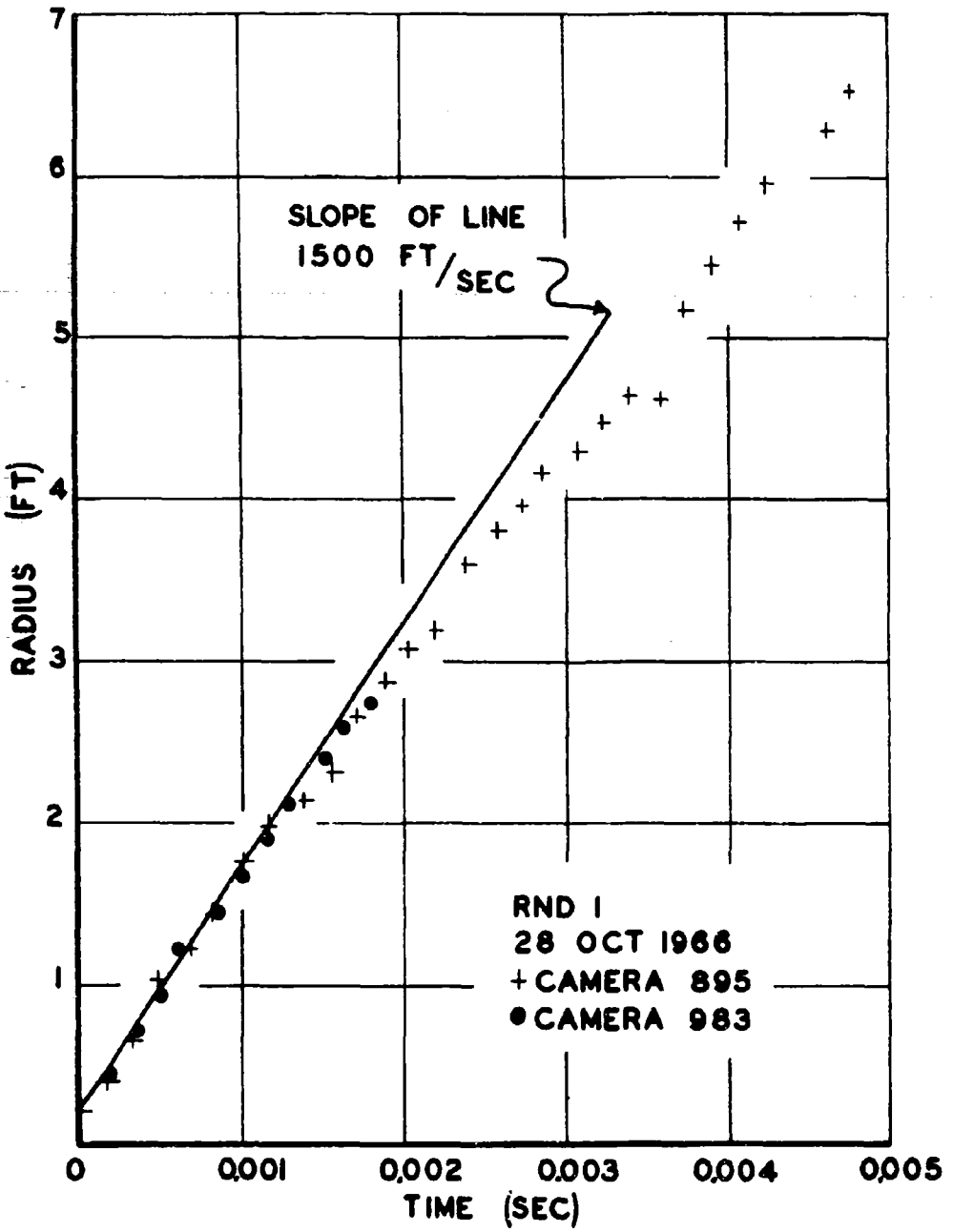

FIG. 5. Shock Wave Radius Three-Pound Device.

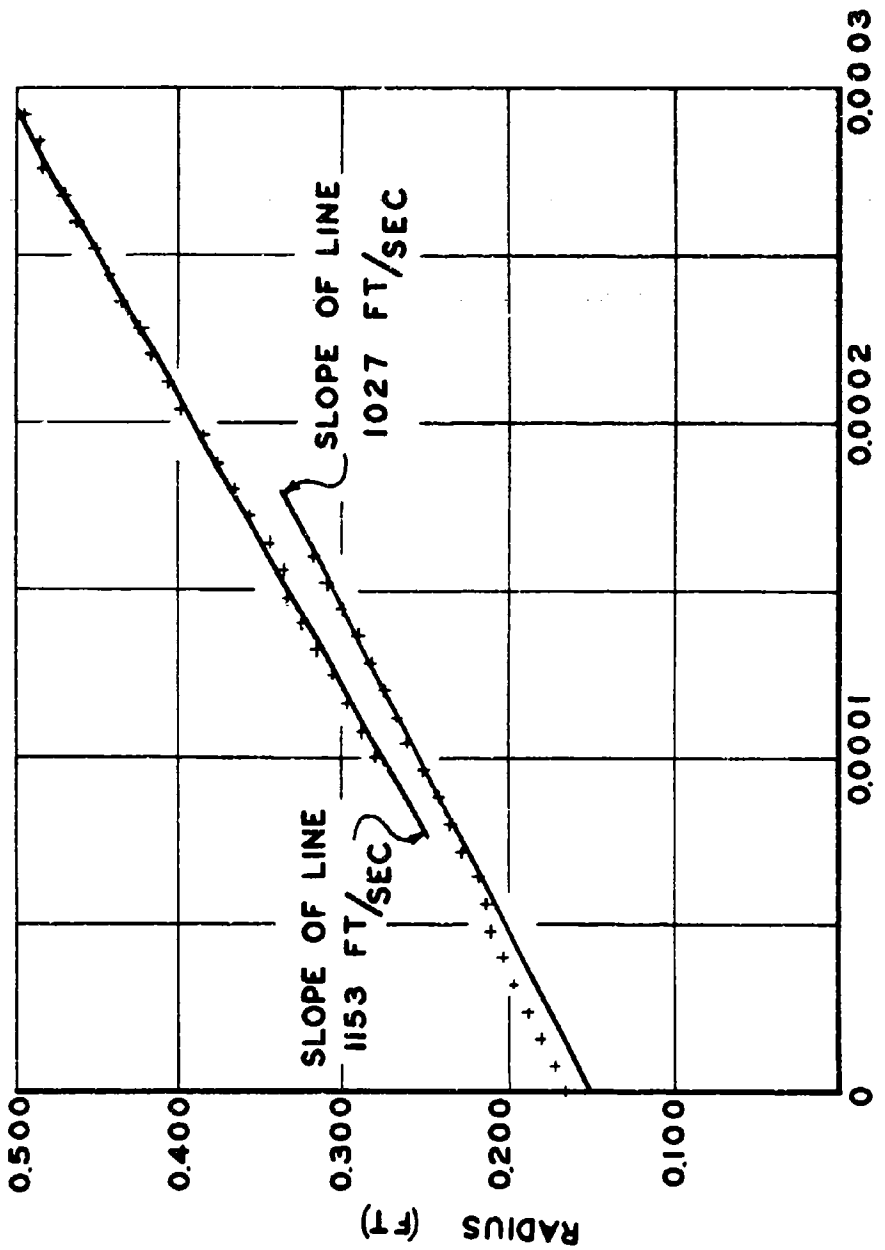

FIG. 6. Initial Fragment Radius Three-Pound Device.

than that in the squirt spikes) follows the fragments outward. Hence, for the three-pound device at least, the initial speed of the main body of the cloud is about 1100 ft/sec. The fragments appear to decelerate slowly as indicated by Fig. 7, which gives typical fragment and cloud distances as a function of time for the first 0.010 seconds. These data were taken from Fastax camera photographs at a framing rate of about 6000 frames per second. Note that the initial average fragment speed must be approximately 1100 ft/sec (as indicated by the Cordin data) for the fragments to reach the point of emergence at the point and time indicated on the Fastax data. This occurs at approximately 3.5 feet and 3 milliseconds. Information is not available on the initial fragment speeds for the larger devices.

SQUIRT SPIKE RADIUS AND SPEED

The squirt spikes have an initial speed greater than that of the fragments since they are projected outward through the cracks in the canister because of a pressure differential between the inside and outside of the canister. Experimental data plotted from Cordin camera frames is illustrated in Fig. 8. It can be seen that for the three-pound device at least, the initial speed of the squirt spikes is about 1225 ft/sec, or some 100 to 150 ft/sec faster than for the fragments of the main body of the cloud.

It is hard to differentiate between the squirt spikes and the main body of the cloud during the first several milliseconds of flight. According to the Fastax data shown in Fig. 9 and 10, which are intended to be for the main body of the cloud, the initial speed of the cloud is about 1250 ft/sec. This compares well with the Cordin data for the squirt spikes. This is because the main body cannot be read during the first few milliseconds and we see only the squirt spikes on the Fastax frames.

MAIN BODY RADIUS AND SPEED

Out to about 3 milliseconds and 3.5 feet radius the position of the main body can't be determined precisely and must be assumed to lie somewhere between the fragments and the squirt spikes. Some of the main body is undoubtedly trapped behind the fragments but some of the main body droplets probably are forced outward between the fragments because of the internal pressure of the expanding detonation products. Thus the main body will have a speed in this period of between 1100 and 1300 ft/sec. Beyond three milliseconds the main body can be differentiated quite well and its position can be plotted as shown in Fig. 9 and 10. Because the difference in speed between the fragments and the squirt spikes is not great (at least for the three-pound device) we have assumed the initial speed of the main body to be that of the squirt spikes.

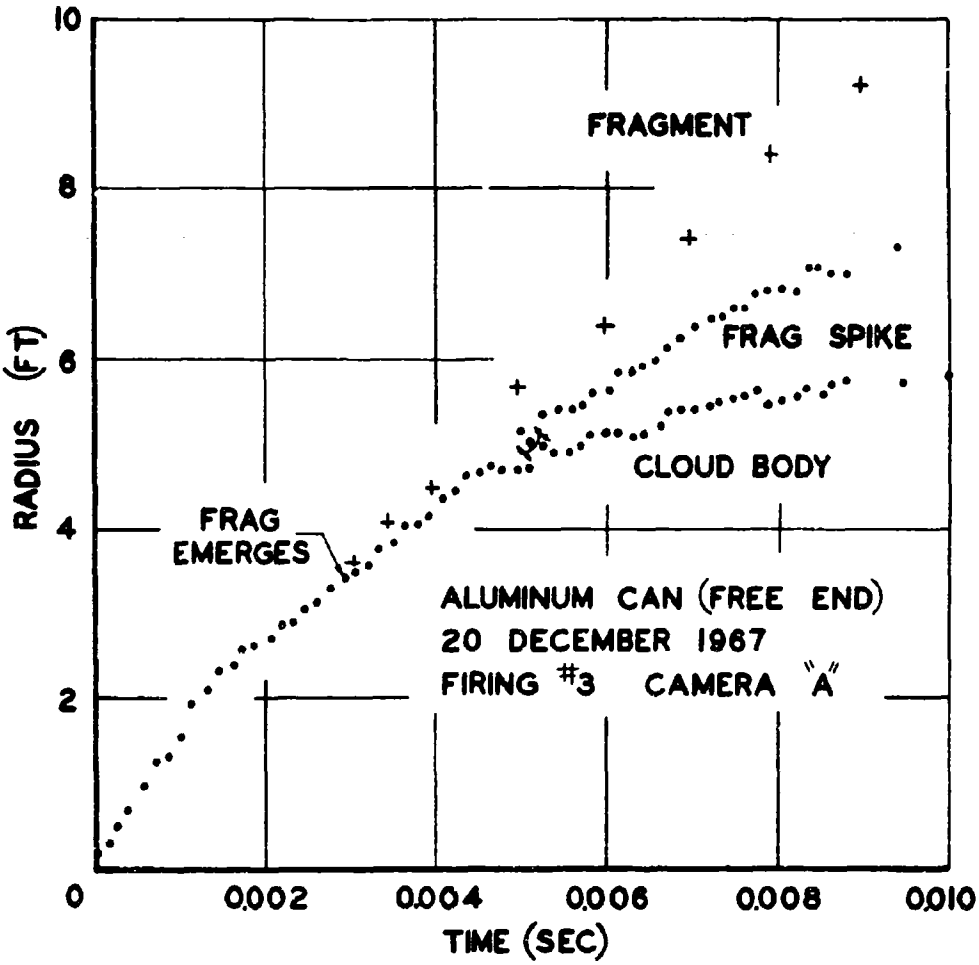

FIG. 7. Fragment and Cloud Radius Three-Pound Device.

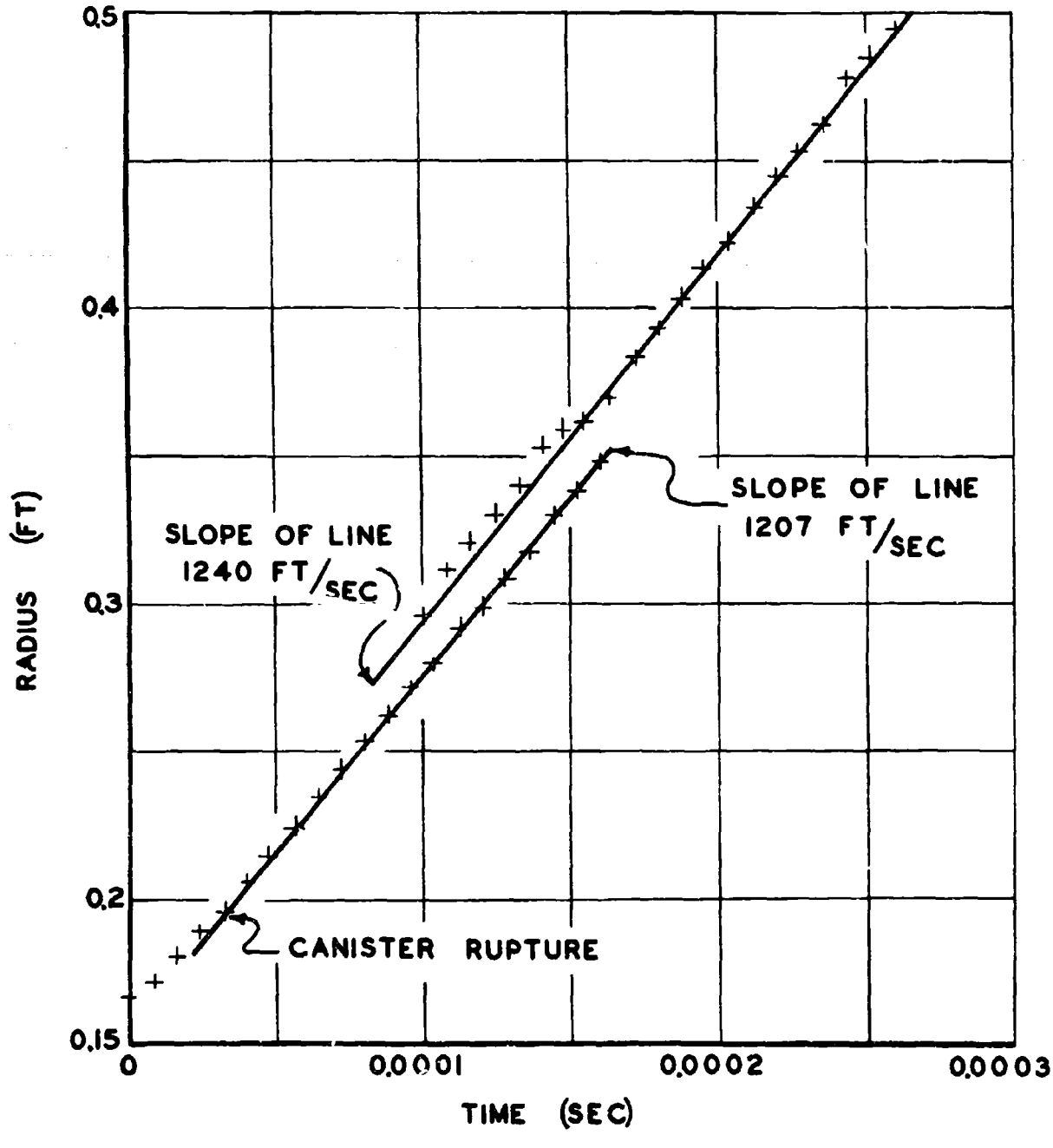

FIG. 8. Initial Cloud (Squirt Spike) Radius Three-Pound Device.

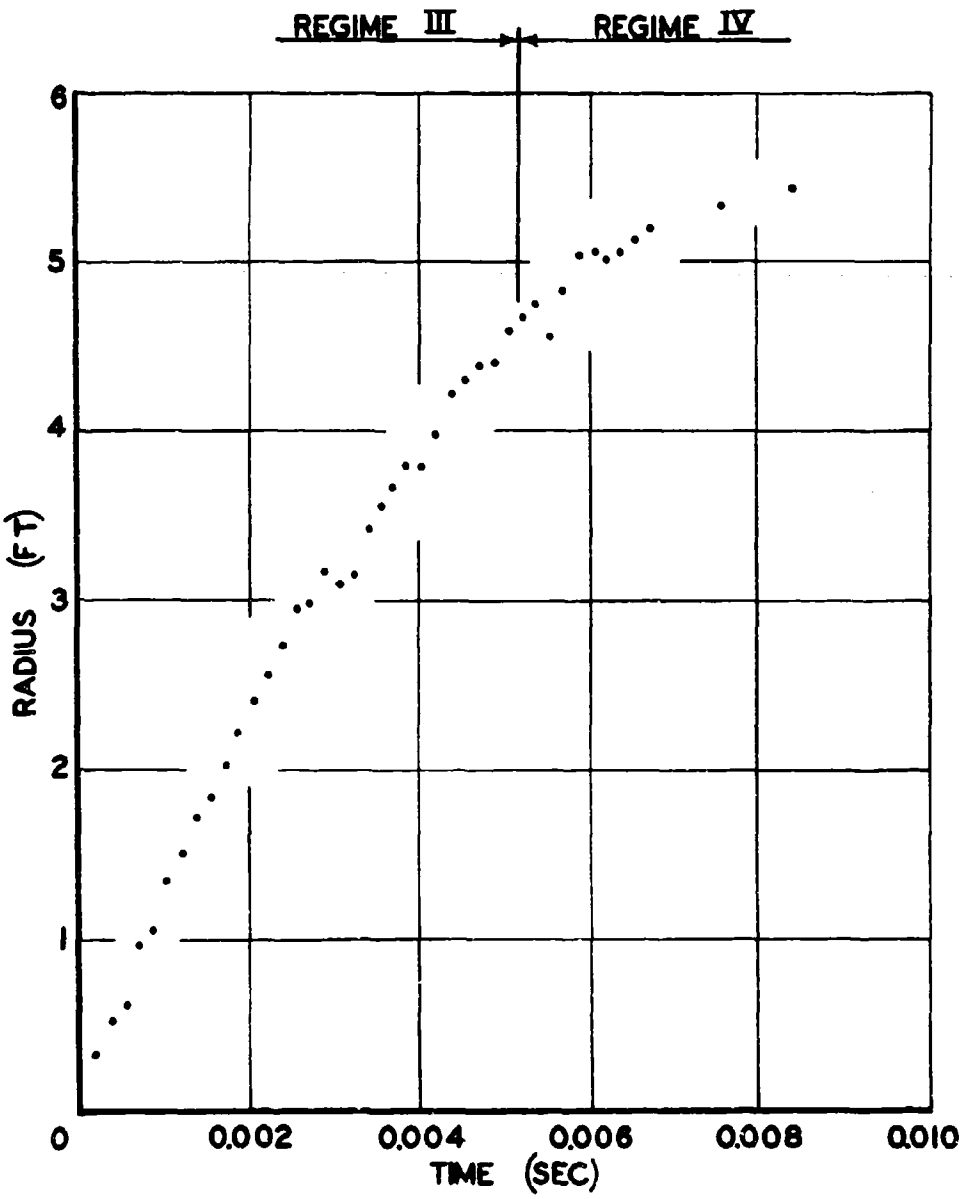

FIG. 9. Cloud Radius to 0.010 Second Three-Pound Device.

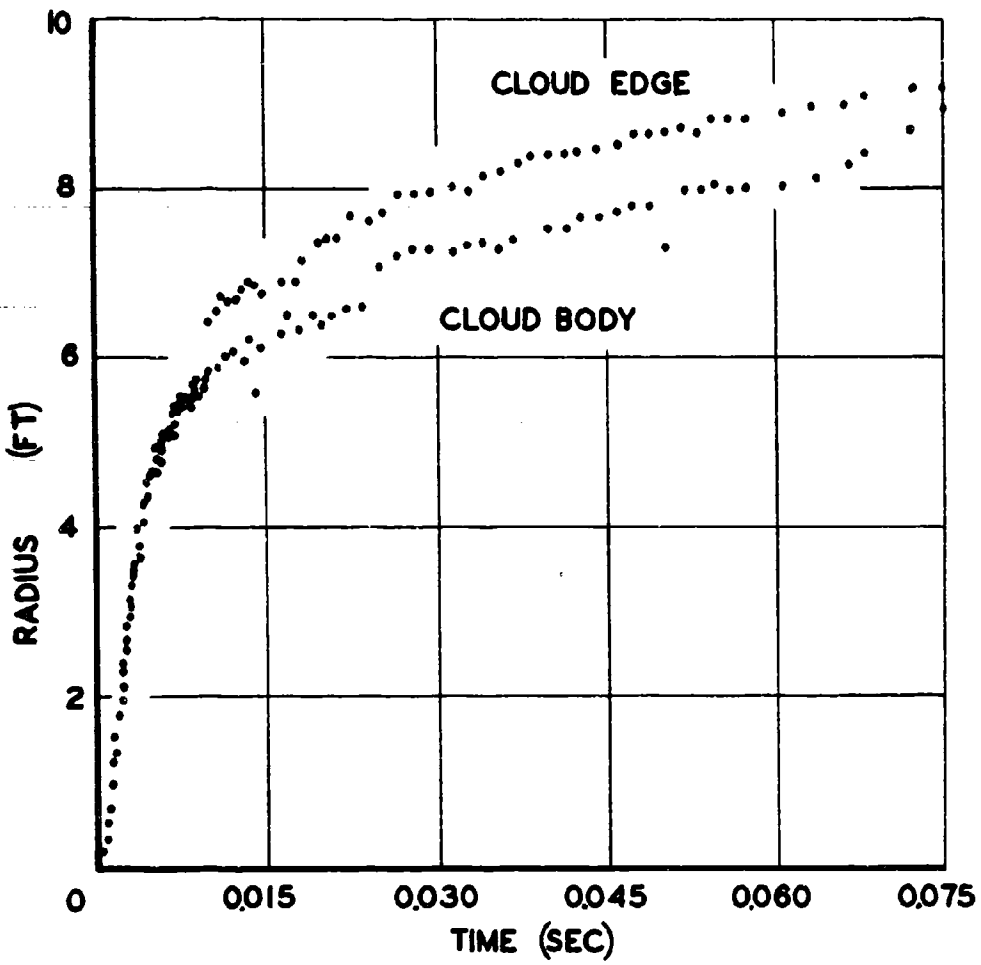

FIG. 10. Cloud Radius to 0.075 Second Three-Pound Device.

Experimental data for speeds as a function of volume for the main body of the cloud are shown in Fig. 11. These data were obtained by graphically measuring the slope of the tangent to the faired radius versus time curve of Fig. 9 at various points. The speed was plotted as a function of cloud volume in order to facilitate comparison with the analytical equation of motion, which was more readily derived as a function of cloud volume. The volume is assumed to be equal to the cloud area times the canister length. For the purposes of the analysis the cloud was assumed to remain constant in thickness during its expansion. We know this is not true, but the error introduced by the assumption is not great and the assumption simplifies the analysis.

The main body radius versus time curve for a typical 83-pound device is shown in Fig. 12. It can be seen that the initial cloud speed appears to be much greater than for the three-pound device. This, we believe, is a result of a much greater initial squirt spike speed for the 83-pound device. The initial slope of the curve appears to be on the order of 2000 ft/sec. This is not unreasonable if we assume that the steel canister of the 83-pound device might rupture before expanding as far as the aluminum canister of the three-pound device. If this were the case the pressure differential between the inside and outside of the steel canister would be much greater than for the aluminum canister at the time of rupture. Hence the squirt speed would be greater for the steel canister.

As will be shown later an initial main body speed of approximately 1380 ft/sec[2] is more reasonable and when that value is used the two devices compare quite well when allowances are made for scaling. Figure 13 shows the main body speed versus cloud volume data for the 83-pound device in which an initial main body speed of 1380 ft/sec is assumed.

ANALYSIS OF CLOUD DISPERSION

PHYSICAL MODEL OF CLOUD DISPERSION

In order to derive equations of motion for the expansion of the explosively dispersed cloud it was necessary to develop a simple model of the dispersion process. We assumed that the device was composed of a cylindrical metal canister filled with liquid as shown in Fig. 1. A cylindrical burster tube extends through the center of the canister and is partially filled with explosive. The presence of the metal of the burster tube is neglected, and the liquid is assumed to fill the remainder of the canister with no allowance for ullage.

[2]This is the initial speed as calculated in a later section.

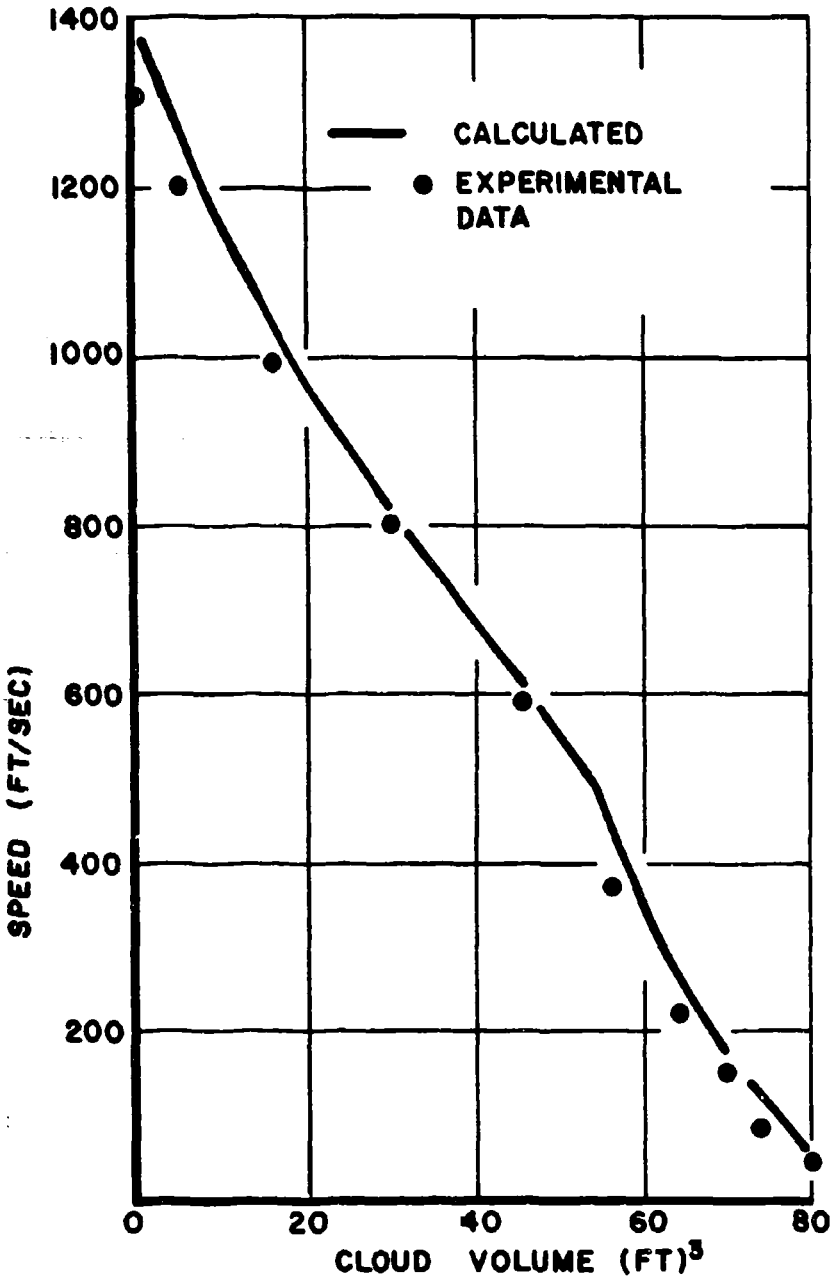

FIG. 11. Cloud Speed as a Function of Volume Three-Pound Device.

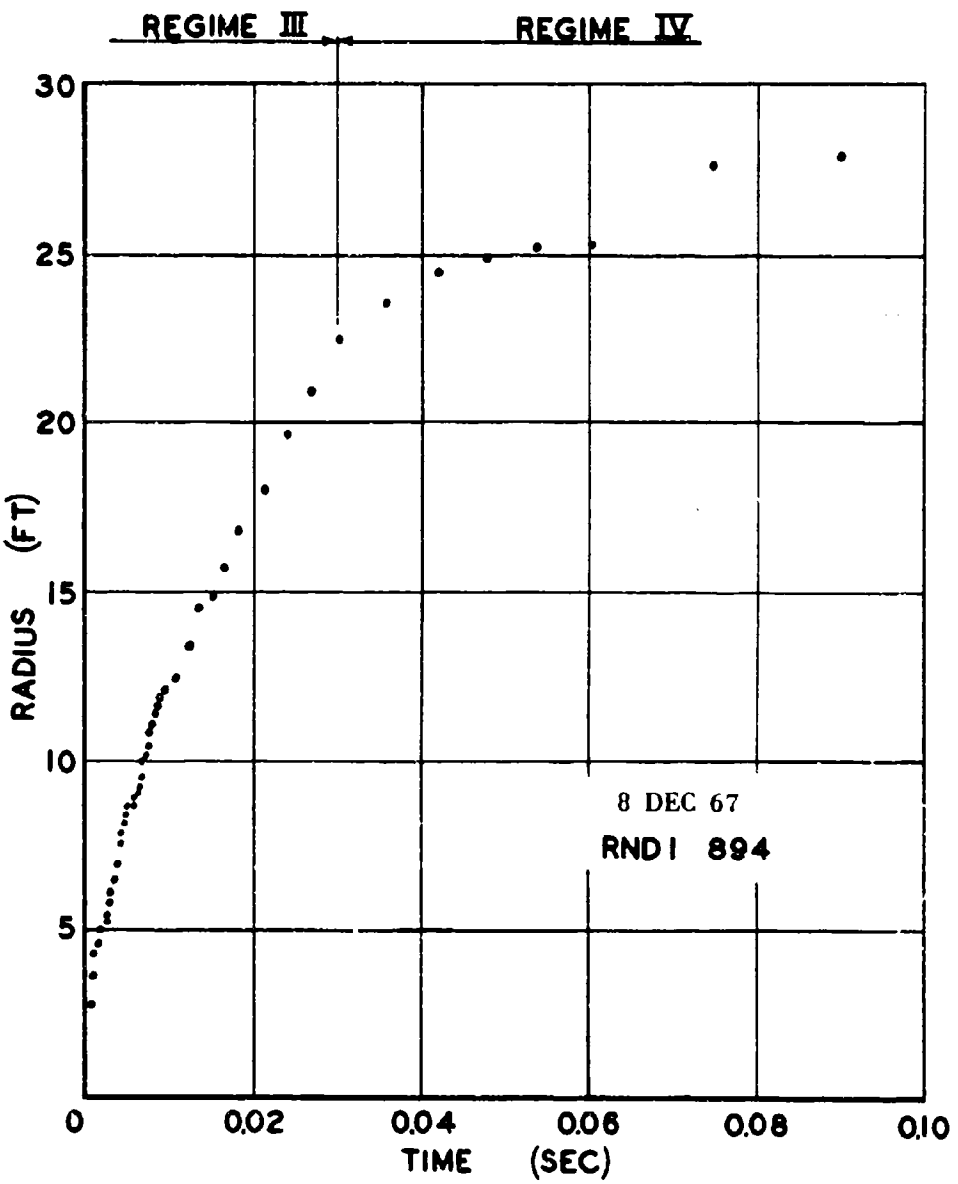

FIG. 12. Main Body Radius as a Function of Time 83 Pound Device.

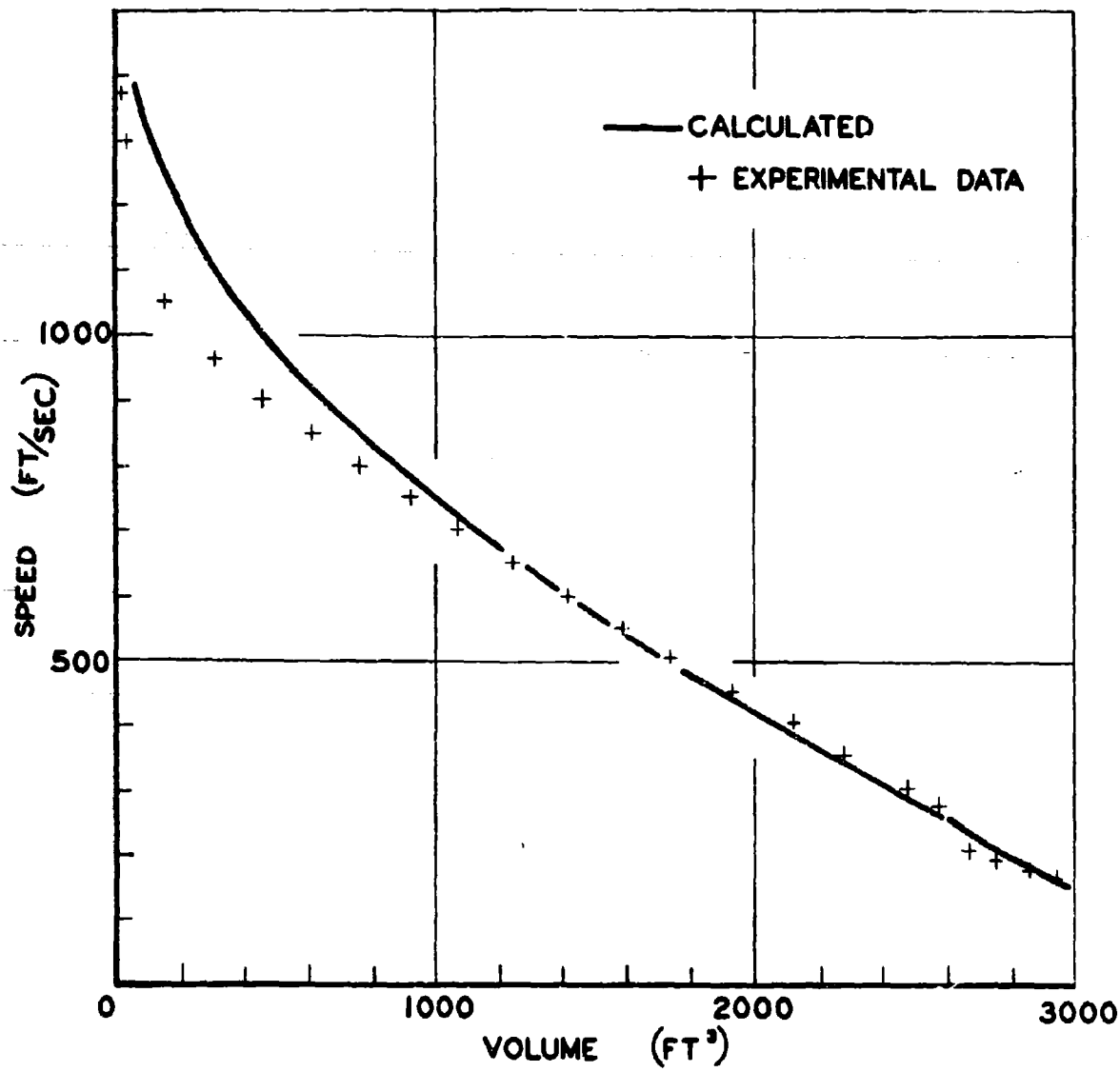

FIG. 13. Cloud Speed as a Function of Volume 83 Pound Device.

The burster explosive is assumed to detonate instantaneously and expand to fill the remainder of the burster column with detonation products. The detonation products then expand radially outward. A detonation wave, preceding the detonation products, is assumed to move radially outward from the burster tube, becoming a shock wave as it enters the liquid. The cylindrical shock wave propagates radially outward from the burster column until it enters the atmosphere surrounding the canister. But, since the strength of the shock wave emerging from the canister is small, we assume that the energy of the detonation is given up entirely to the liquid and fragments.

The liquid is assumed to expand radially outward. As noted previously, we assume that the cloud does not increase in thickness during the expansion process, but remains equal in thickness to the length of the canister.

To simplify the analysis we have divided the dispersion process into several regimes, each of which will be treated separately. This is necessary because the physical processes governing each regime are different so that it is only reasonable to expect that different equations of motion will be required. We have attempted to develop equations of motion which will grossly predict the behavior of the cloud without undue complexity. As we gain further understanding of the phenomena involved it will be possible to refine or rework the analysis to provide a more exact model.

INITIAL REGIME

The Initial Regime is assumed to begin when the burster explosive detonates. During this regime the burster explosive is transformed from solid explosive filling a portion of the burster tube to detonation products at very high temperature and pressure completely filling the burster tube.

Knowing the detonation pressure and the initial volume, which is assumed to be the initial volume of the solid explosive, we can determine the pressure of the detonation products at the end of the Initial Regime by means of the polytropic equation for the gas:

$$P_{og} = P_{dg} \left(\frac{V_{dg}}{V_{og}} \right)^n \qquad (1)$$

where

n = polytropic exponent

P_{og} = gas pressure at the end of the Initial Regime

P_{dg} = detonation pressure of the explosive

V_{og} = gas volume at the end of the Initial Regime

V_{dg} = solid explosive volume at detonation

According to Ref. 4 the polytropic exponent is about 3.0 at the time of detonation but decreases rapidly. We will assume an average value of n = 2.0 for the Initial Regime. The detonation pressure of a typical explosive, from Ref. 4, is 87,000 atm or 1.84×10^8 psf.

Three-Pound Device

For a typical three-pound device the solid explosive, as can be seen from Table 1, fills half the burster tube so that $V_{og} = 2V_{dg}$. Substituting in Eq. 1 we get

$$P_{og} = (1.84 \times 10^8)\ (0.5)^2 = 4.6 \times 10^7 \text{ psf}$$

Eighty-Three Pound Device

The detonation pressure and the average value of n were assumed th same for the 83-pound device as for the three-pound device. From Table 1 the remaining initial conditions are:

$$V_{dg} = 7.29 \times 10^{-3} \text{ ft}^3$$

$$V_{og} = 8.11 \times 10^{-3} \text{ ft}^3$$

Substitution of the above values in Eq. 1 results in a final pressure:

$$P_{og} = 1.49 \times 10^8 \text{ psf}$$

This pressure is three times that of the three-pound device because the free volume in the burster tube for the 83-pound device is proportionately much less than in the three-pound device.

REGIME I

Regime I begins when the burster tube begins to expand, forcing the liquid and canister walls outward. We assume that the shock wave from the detonation imparts negligible speed to the liquid, which is forced outward solely by the pressure of the expanding detonation products. The canister walls are forced outward in turn by the liquid. In this

regime the gaseous detonation products are forced to expand against the inertia of the liquid and the canister walls, the resistance of the stretching canister walls, and the pressure of the surrounding atmosphere.

We assume that the canister walls expand so that the canister remains cylindrical and its length remains constant. It is further assumed that no liquid vaporizes during the process.

When the metal of the canister reaches its ultimate elongation, the canister ruptures along the longitudinal grooves, signifying the end of Regime I.

In this regime we assume our system (or control volume) to be the liquid cylinder which is being dispersed. It is bounded on the inside by the expanding detonation products and on the outside by the walls of the cylinder and the ends of the canister (see Fig. 14).

Equation of Motion

The energy equation for a non-flow system is the basis for the equation of motion. We assume that no mass is transferred across the system boundaries and that heat transfer and changes in potential, internal, and chemical energy are negligible. The only work done on or by the system is expansion work so that the energy equation becomes

$$- \delta W_{exp.} = dE_k \tag{2}$$

where E_k is the average kinetic energy of the liquid mass. It is assumed to be given by the relation

$$dE_k = m_\ell v_a dv \tag{3}$$

where

m_ℓ = mass of the liquid = constant

v_a = average speed through the liquid shell

The expansion work is composed of three parts; the work done on the liquid by the expanding detonation products, the work done by the liquid in expanding the metal canister, and the work done by the liquid in pushing aside the atmosphere. In this regime, since the work done in expanding the canister is much greater than the atmospheric work, the latter can be neglected.

The work done on the system by the detonation products is given by the relation

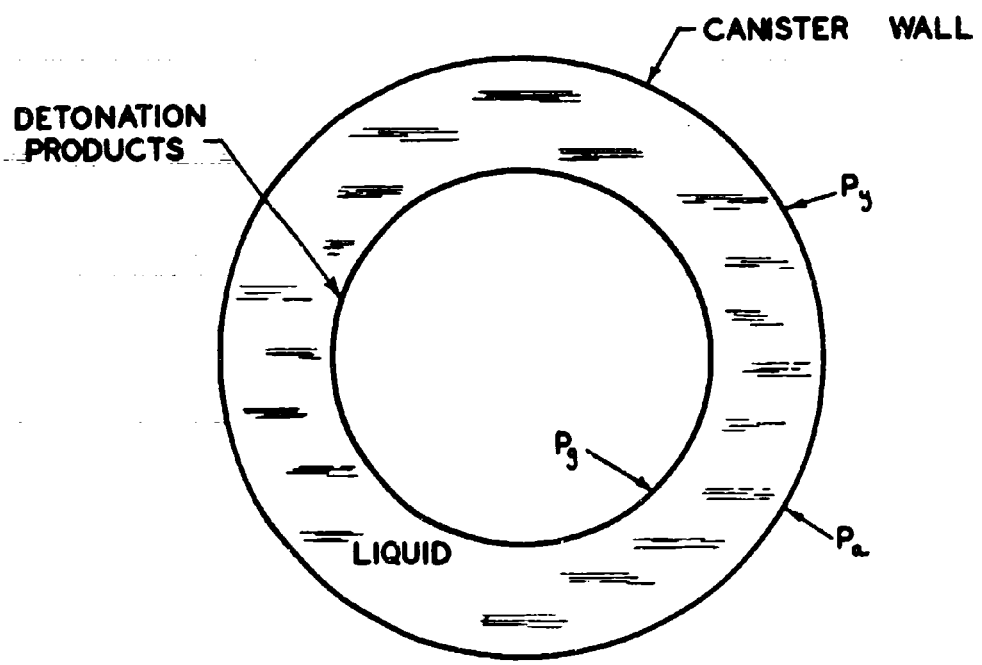

FIG. 14. Control Volume.

$$W_g = - \int P_g dV_g$$

where

P_g = pressure of the gaseous detonation products

V_g = volume of the gaseous detonation products

The gas pressure varies as a function of the gas volume. If we assume a polytropic expansion for the gas then

$$P_g = P_{og} \left(\frac{V_{og}}{V_g} \right)^n$$

This can be substituted into the gas expansion work term to give

$$- \int P_g dV_g = - P_{og} V_{og}^{\ n} \int V_g^{-n} dV_g \tag{4}$$

The work done on the canister by the system is given by

$$W_p = \int P_y dV_p \tag{5}$$

where

P_y = pressure required to exceed the metal yield stress

V_p = volume of the canister

Substitution of relations (3), (4), and (5) into Eq. 2 gives the differential form of the equation of motion for Regime I which is

$$- \int_{V_{op}}^{V_p} P_y dV_p + P_{og} V_{og}^{\ n} \int_{V_{og}}^{V_g} V_g^{-n} dV_g = \int_o^{v_a} m_\ell v_a dv$$

Since the mass of the liquid is constant and if we assume the pressure required to expand the metal to be a constant the equation of motion can be integrated directly to give

$$-P_y (V_p - V_{op}) + \frac{P_{og} V_{og}^{n}}{1-n} (V_g^{1-n} - V_{og}^{1-n}) = \frac{m_\ell}{2} v_a^2$$

or

$$v_a^2 = \frac{2}{m_\ell} \left[\frac{P_{og} V_{og}^{n}}{1-n} (V_g^{1-n} - V_{og}^{1-n}) - P_y (V_p - V_{op}) \right] \qquad (6)$$

Since we are interested in the speed of the leading edge of the cloud rather than in the average speed of the cloud as given by the above relation, we assume a volume relation for the system (see Fig. 15), such that

$$\pi L (r^2 - r_a^2) = \frac{V_\ell}{2} = \text{const.}$$

where

L = canister length

r = outside radius of liquid shell

r_a = radius at which v_a occurs

Therefore, half of the liquid volume is at a greater radius than r_a, and half is at a lesser radius.

Differentiating with respect to time we have

$$2\pi L \left(r \frac{dr}{dt} - r_a \frac{dr_a}{dt} \right) = 0$$

or

$$v_a = \frac{r}{r_a} v$$

since

$$v_a = \frac{dr_a}{dt} \qquad v = \frac{dr}{dt}$$

Note that the average cloud speed is greater than the speed of the edge of the cloud. The liquid particles nearer the center of the cloud must be moving faster than those near the edge because the radius of the cloud is increasing but the liquid volume is assumed to remain constant. This is illustrated in Fig. 16.

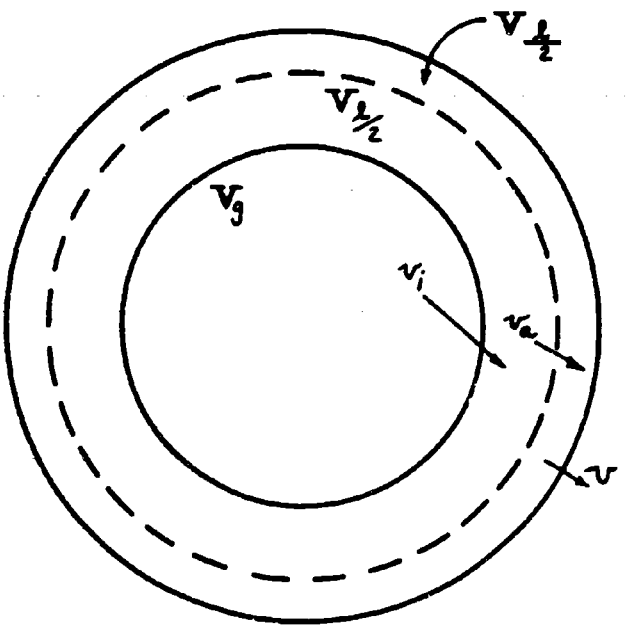

FIG. 15. Volume Relations.

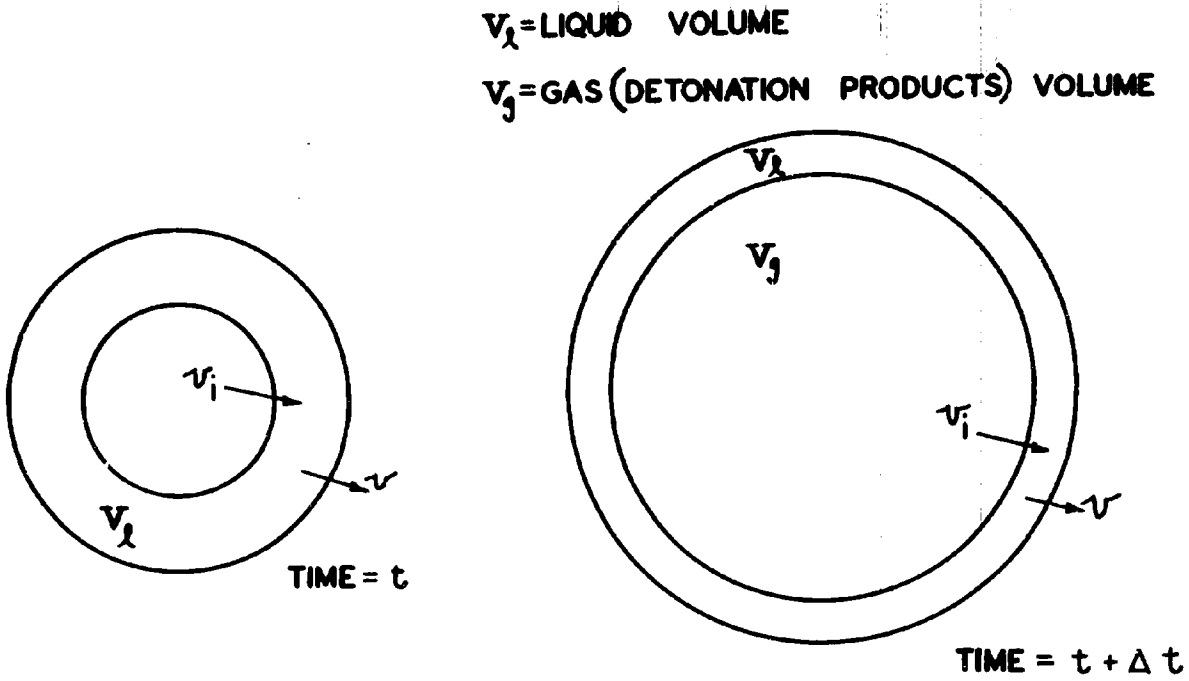

FIG. 16. Speeds of Liquid Particles.

By substitution, the relation between the average cloud speed and the speed of the edge of the cloud can be expressed in terms of volumes (see Fig. 15).

$$v_a = v \sqrt{\frac{V_p}{V_g + \frac{V_\ell}{2}}}$$

Equation 6 can further be simplified by noting that

$$V_g^{1-n} << V_{og}^{1-n}$$

so that the former term can be neglected at $t_o + \Delta t$.

Furthermore

$$V_g = V_p - V_\ell$$

so that the equation of motion for Regime I becomes finally

$$v^2 = \frac{2V_p - V_\ell}{m_\ell V_p} \left[\frac{P_{og} V_{og}}{n-1} + P_y (V_{op} - V_p) \right] \qquad (7)$$

Yield Pressure

In order to determine the yield pressure of the metal (P_y) we assume that the relation for the hoop stress in a thin wall cylinder is applicable:

$$P_y = S_y \frac{t}{r}$$

where

S_y = stress at which metal yields

P_y = pressure at which metal yields

r = canister radius

t = canister thickness

If we assume the following values for a typical three-pound device

S_y = 35,000 psi t = 0.050 inch (in groove) r = 2 inches

the yield pressure is calculated to be 875 psi or 1.26×10^5 psf.

Calculation of Speed in Regime I

The maximum expansion speed in Regime I can be calculated by the use of Eq. 7 since we know or can calculate all the required values except the polytropic exponent, n. We don't know the relationship between n and the gas volume. We can, however, determine an average value of n by noting that the assumed value of n was 2.0 in the Initial Regime and that its value approaches 1.2 as the detonation products approach perfect gas conditions. We will assume an average value of n = 1.6.

The final volume can be obtained by assuming a linear elongation before breakage for the metal of the canister. The final volume[3] is given by

$$V_{Ip} = V_{op}\,\varepsilon^2 \qquad \varepsilon = \text{maximum elongation}$$

Three-Pound Device

The values required for substitution in Eq. 7 are obtained from Table 1:

$$V_\ell = m_\ell/\rho_\ell = 5.18 \times 10^{-2}\ \text{ft}^3$$

$$V_{og} = 11.4 \times 10^{-4}\ \text{ft}^3$$

$$V_{op} = V_{og} + V_\ell = 5.29 \times 10^{-2}\ \text{ft}^3$$

$$P_{og} = 4.6 \times 10^7\ \text{psf}$$

$$m_\ell = 0.093\ \text{slug}$$

$$P_y = 1.26 \times 10^5\ \text{psf}$$

If the maximum linear elongation is assumed to be 1.2 then the final volume is given by:

$$V_{Ip} = \varepsilon^2 V_{op} = (1.2)^2\,(5.29 \times 10^{-2}) = 7.62 \times 10^{-2}\ \text{ft}^2$$

[3]The subscript (I) denotes the end of Regime I.

These values can be substituted in Eq. 7 to give

$$v^2 = \frac{2(7.62 \times 10^{-2}) - 5.18 \times 10^{-2}}{0.093(7.62 \times 10^{-2})} \left[\frac{(4.6 \times 10^{7})(11.4 \times 10^{-4})}{1.6-1} + (1.26 \times 10^{5})(5.29 \times 10^{-2} - 7.62 \times 10^{-2})\right]$$

Simplification then gives

$$v^2 = 1.20 \times 10^{6} \text{ ft}^2/\text{sec}^2$$

or

$$v = 1100 \text{ ft/sec}$$

This is nearly the experimentally determined speed of the fragments as they leave the canister as illustrated by Fig. 6. The value of v is strongly influenced by the value of the polytropic constant, n. Had we chosen values of 1.5 or 1.7 (6% change) for n, the calculated speed would have varied by about 10% which would still be a reasonable value for v.

Eighty-Three Pound Device

The initial values required for insertion in the equation of motion are taken from Table 1 as follows:

$$V_{\ell} = m_{\ell}/\rho_{\ell} = 1.43 \text{ ft}^3$$

$$V_{og} = V_b = 14 \text{ in}^3 = 8.11 \times 10^{-3} \text{ ft}^3$$

$$V_{op} = V_{og} + V_{\ell} = 1.44 \text{ ft}^3$$

$$P_{og} = 1.49 \times 10^{8} \text{ psf}$$

$$m_{\ell} = 2.59 \text{ slugs}$$

The canister yield pressure (P_y) is calculated from the equation for hoop stress and has a value of 370 psi or 5.33×10^4 psf based on the following canister characteristics:

Yield stress:	50,000 psi
Thickness of metal:	0.050 inches
Canister radius:	6.75 inches

As will be shown later, the maximum linear elongation prior to rupture of the metal in the canister must be about 1.025 in order to satisfy the experimental data so that

$$V_{Ip} = \varepsilon^2 V_{op} = (1.025)^2 (1.44) = 1.513 \text{ ft}^3$$

Substitution of the above values into Eq. 7 gives

$$v^2 = \frac{2(1.51) - 1.43}{2.59(1.51)} \left[\frac{(1.49 \times 10^8)(8.1 \times 10^{-3})}{1.6-1} + 5.33 \times 10^4 (1.44 - 1.51) \right]$$

which, on simplification, gives

$$v^2 = 8.18 \times 10^5 \text{ ft}^2/\text{sec}^2$$

or

$$v = 904 \text{ ft/sec}$$

This value is about 200 ft/sec slower than that calculated for the three-pound device, the difference being primarily a result of the lower burster charge-to-liquid ratio used for the 83-pound device and the lower value of elongation which was assumed for the 83-pound device.

Gas Pressure at the End of Regime I

As a further check we can calculate the gas pressure of the detonation products at the end of Regime I by the use of the polytropic equation for the gas

$$P_{Ig} = P_{og} \left(\frac{V_{og}}{V_{Ig}} \right)^n$$

Three-Pound Device

Substitution of the appropriate values for the pressure and volume gives

$$P_{Ig} = 4.6 \times 10^7 \left(\frac{11.4 \times 10^{-4}}{2.44 \times 10^{-2}} \right)^{1.6}$$

$$P_{Ig} = 3.42 \times 10^5 \text{ psf}$$

or

$$P_{Ig} = 2370 \text{ psi}$$

This value of the pressure is in the right range to give the observed speed of the squirt spikes as shown in the next section.

Eighty-Three Pound Device

The value for the pressure at the end of Regime I is given by the polytropic equation where

$$V_{Ig} = V_{Ip} - V_{\ell} = 1.513 - 1.430 = 0.083 \text{ ft}^3$$

$$P_{Ig} = 1.49 \times 10^8 \left(\frac{8.10 \times 10^{-3}}{0.083}\right)^{1.6}$$

$$P_{Ig} = 3.6 \times 10^6 \text{ psf}$$

$$P_{Ig} = 25{,}000 \text{ psi}$$

This is considerably more than the value calculated for the three-pound device. If we refer to the experimental radius versus time curves for the two devices (Fig. 8 and 12) it can be seen that the initial squirt jet speed for the 83-pound device appears to be much greater than the three-pound device. In fact, the initial squirt jet speed for the 83-pound device appears to be almost 2000 ft/sec as compared to some 1225 ft/sec for the smaller device. In order that this might be so, the canister pressure at the end of Regime I for the 83-pound device would have to be on the order of 25,000 psi as will be shown later. This could be so if the canister ruptured sufficiently early, since the internal pressure would be much greater under those conditions at the time of rupture.

Squirt Jet Speed

The initial speed of the squirt jets can be approximated from the orifice equation:

$$v_s = C_d \sqrt{\frac{2\Delta P}{\rho_{\ell}}}$$

where

C_d = discharge coefficient (empirical)

ρ_{ℓ} = liquid density (slugs per cubic foot)

ΔP = pressure drop across the orifice (lb/ft^2)

For this particular case the pressure drop can be assumed equal to the pressure of the detonation products minus the atmospheric pressure at the time of rupture.

Three-Pound Canister

The stagnation pressure of the air outside the canister is approximately two atmospheres or 2000 psf at the time of rupture. The pressure drop is thus given by

$$\Delta P = P_{Ig} - P_a = 3.42 \times 10^5 - 0.02 \times 10^5 = 3.40 \times 10^5 \text{ psf}$$

If the discharge coefficient is assumed to be 0.5 (which is only a guess) and the liquid density is 1.80 slugs/ft^3 then

$$v_s = 0.5 \sqrt{\frac{2(3.40 \times 10^5)}{1.80}}$$

$$v_s = 300 \text{ ft/sec}$$

The speed of the jet is then the squirt speed plus the fragment or cloud speed

$$v_j = v_s + v = 300 + 1100$$

$$v_j = 1400 \text{ ft/sec}$$

This is to be compared to the measured initial speed of the squirt spikes which is about 1225 ft/sec (see Fig. 8).

Eight-Three Pound Device

The lack of available information for this device makes it difficult to analyse the squirt jet speed. The cloud speed and the pressure at the end of Regime I which we obtained in the earlier section do not agree with the experimental data which we have available. But, if we assume that the experimental data is correct and assume a squirt spike speed of about 2000 ft/sec, the pressure drop required to give this speed can be determined from the orifice equation. If we assume the speed of the fragments to be 1000 ft/sec the speed of the jet emerging from the canister is

$$2000 - 1000 = 1000 \text{ ft/sec}$$

The orifice equation is arranged in the form

$$\Delta P = \left(\frac{v_s}{C_d}\right)^2 \frac{\rho_\ell}{2}$$

Substitution of the appropriate values gives

$$\Delta P = \left(\frac{1000}{0.5}\right)^2 \frac{1.8}{2} = 3{,}600{,}000 \text{ psf}$$

$$\Delta P = 25{,}000 \text{ psi}$$

Elongation of the Canister

We can determine the maximum canister elongation which would give the above pressure at the time of rupture. Knowing the initial and final pressures and the initial volume we can calculate the final volume by the polytropic equation.

$$V_{Ig} = \left(\frac{P_{og}}{P_{Ig}}\right)^{1/n} V_{og}$$

Substituting the appropriate values we get

$$V_{Ig} = \left(\frac{1.49 \times 10^8}{3.6 \times 10^6}\right)^{1/1.6} 8.1 \times 10^{-3} = (41.4)^{0.625} (8.1 \times 10^{-3})$$

$$V_{Ig} = 8.3 \times 10^{-2} \text{ ft}^3$$

The elongation of the canister is given by the equation

$$\varepsilon = \sqrt{\frac{V_{Ip}}{V_{op}}}$$

where

$$V_{Ip} = V_{Ig} + V_{\ell} = 8.3 \times 10^{-2} + 1.43 = 1.51 \text{ ft}^3$$

$$V_{op} = 1.44 \text{ ft}^3$$

so that

$$\varepsilon = \sqrt{\frac{1.51}{1.44}} = \sqrt{1.05} = 1.025$$

This suggests that either the canister is rupturing almost instantaneously without stretching appreciably (possibly as a result of impulsive loading) or that the squirt speed measured from Fig. 12 is wrong. The characteristics of aluminum and steel under impulsive loads provide evidence, however,

that the steel canister might well rupture earlier than the aluminum canister. Reference 5, for example shows that the critical impact velocity for aluminum is about twice that for steel:

Material	Critical Impact Velocity
24ST Aluminum	200+ ft/sec
1020 Steel	100 ft/sec

The critical impact velocity is the speed at which a material shatters at the point of impact. As such it is a measure of the resistance of a metal to shattering under an impulsive load such as a detonation wave. The lower value of critical impact velocity for steel indicates that it is more likely to shatter under a given impulsive load than is aluminum.

If the canister of the 83-pound device does rupture at an elongation of only 1.025 then the fragment speed at the end of Regime I will be lower than for the three-pound device. We know that the fragments of the 83-pound device do travel considerably further than the fragments for the three-pound device. This can be explained by the greater mass per unit area of the steel fragments of the 83-pound device as compared with the aluminum fragments of the three-pound device. It might be informative to determine experimentally the distance traveled by fragments from, say, a steel-walled three-pound canister or an aluminum-walled 83-pound canister.

REGIME II

During Regime II we assume that a "fluid piston" composed of the still expanding detonation products, the liquid shell surrounding the gaseous products, and the metal canister fragments governs the outward expansion. The fluid piston is assumed to be a coherent mass and the liquid surrounding the detonation products is assumed not to have broken into discrete droplets, but is able to contain the detonation gases within it. The average speed of the expanding cloud is increasing during this regime because the net expansion force is positive. The gas pressure is greater than the atmospheric pressure and there is an outward acceleration of the liquid.

During Regime II the cloud is divided into two distinct parts which expand at different rates. They are:

1. The squirt spikes are assumed to instantaneously reach their maximum speed at the beginning of Regime II and then to decelerate as a result of aerodynamic drag in the disturbed atmosphere behind the propagating shock wave. The liquid in the squirt spikes is assumed initially to be in the form of a jet of liquid being forced outward through an orifice formed by the separating walls of the canister.

2. The main Body of the cloud is assumed to be the remainder of the liquid between the fragments and the squirt spikes. Initially it is assumed to be a coherent mass which contains the detonation products within it. Gradually it breaks up into droplets, but in this regime the droplets are packed sufficiently close together so that they entrain any air between them and continue to act as a coherent mass.

In this regime we assume the speed of the edge of the main body to be the speed the main body would achieve if it were not restrained by the fragments. The main body of the cloud is forced outward by the pressure of the detonation products and in turn the main body presses outward against the fragments and the atmosphere. The main body also presses outward against the droplets comprising the squirt spikes, an effect which is assumed to be negligible.

We assume that the entire mass of the main body moves uniformly outward and that any atmospheric air which is entrained moves outward at the same speed as the liquid. We further assume that the volume of the cloud is the same as the original liquid volume[4] and that the cloud expands only in the radial direction (i.e., the height of the cloud remains constant and equal to the original canister length).

At the beginning of Regime II, when the canister ruptures, the strips move outward at approximately the same initial speed as the main body of the cloud. We assume that during Regime II the fragments accelerate more slowly than the droplets comprising the main body of the cloud since they are more massive. Thus a portion of the cloud reaches a greater maximum speed than the fragments. A problem arises here since Regime II extends outward to only two or three canister radii. Therefore, a considerable portion of the main body may be trapped behind the fragments and cannot accelerate more rapidly than the fragments. We will assume that the speed of the main body is the speed which the main body would achieve if it were not restrained by the fragments. Note that even though the speed of the leading edge of the cloud might be restrained from increasing markedly by the fragments, the average speed of the cloud can still increase markedly because the droplets closer to the center must travel faster than the droplets nearer the outer edge in order to satisfy the condition that the liquid volume remain constant.

Regime II begins at the point of canister rupture and continues to the point at which the main body of the cloud reaches its average maximum speed.

In this regime the canister has ruptured so the canister expansion work term disappears from the equation of motion. Furthermore, the liquid which has squirted out through the breaks in the canister wall

[4] In order to maintain a constant volume liquid shell, the thickness of the liquid shell decreases as the radius of the system increases.

must be accounted for in terms of lost mass and lost energy since we assume these squirt spikes to be independent of the main body of the cloud. A control volume similar to that postulated for Regime I is used.

Equation of Motion

The energy equation for a non-flow system, which is again used as the basis for the equation of motion, can be written

$$\int P_g \, dV_g - \int P_{as} dV_p = m_{\ell p} \int v dv + E_s$$

where

P_{as} = atmospheric pressure at the face of the piston[5]

E_s = energy lost to the squirt spikes

$m_{\ell p}$ = mass of liquid in fluid piston

We integrate from the point of canister rupture ($_I$) to the point of maximum speed and the end of Regime II ($_{II}$). After substitution of the polytropic relation

$$P_g = P_{Ig} \left(\frac{V_{Ig}}{V_g} \right)^n$$

we get the equation

$$\frac{P_{Ig} V_{Ig}}{1-n}^n \left(V_g^{1-n} - V_{Ig}^{1-n} \right) - P_{as}(V_p - V_{Ip}) = \frac{m_{\ell p}}{2} \left(v_a^2 - v_{Ia}^2 \right) + E_s$$

The speed v_a is the average speed of the liquid mass at any volume, V. Solving for the square of the speed, v_a^2, we get

$$v_a^2 = \frac{2}{m_{\ell p}} \left[\frac{P_{Ig} V_{Ig}}{1-n}^n (V_g^{1-n} - V_{Ig}^{1-n}) - P_{as}(V_p - V_{Ip}) - E_s \right] + v_{Ia}^2$$

[5] P_{as} is a function of the cloud speed since it is the stagnation pressure at the face of the piston. Since the speed is fairly constant in this Regime we will assume P_{as} to be constant to simplify the integration.

Since we want the speed of the edge of the cloud rather than the average speed we substitute

$$v_a = \frac{r}{r_a} v = \sqrt{\frac{V_p}{\frac{V_\ell}{2} + V_g}} \quad v$$

to get the equation of motion for Regime II:

$$v = \sqrt{\frac{\frac{V_\ell}{2} + V_g}{V_p} \left\{ \frac{2}{m_{\ell p}} \left[\frac{P_{Ig} V_{Ig}^{\,n}}{1-n} \left(V_g^{\,1-n} - V_{Ig}^{\,1-n} \right) - P_{as} \left(V_p - V_{Ip} \right) - E_s \right] + \left(\frac{V_{Ip}}{\frac{V_\ell}{2} + V_{Ig}} \right) v_I^{\,2} \right\}} \qquad (8)$$

Energy Lost to Squirt Spikes

The energy lost to the squirt spikes is a function of the squirt spike speed and the mass of the liquid in the squirt spikes.

Three-Pound Device

The speed of the squirt spikes, v_j, was calculated in an earlier Section as 1400 ft/sec. We don't know the mass of liquid in the squirt spikes, but estimate it to be about 10% of the total liquid mass, or

$$m_{\ell s} = 0.1 m_\ell = 0.1(0.093 \text{ slug}) = 0.0093 \text{ slug}$$

The energy lost to the squirt spikes is then

$$E_s = \frac{m_{\ell s}}{2} \left(v_j^{\,2} - v^2 \right)$$

where

v_j = squirt spike speed

v = main body speed

substituting numerical values we get

$$E_s = \frac{0.0093}{2} \left(1400^2 - 1100^2 \right)$$

$$E_s = 3500 \text{ ft-lb}$$

Eighty-Three Pound Device

If we again say that 10% of the total liquid mass goes into the squirt spikes the energy lost is given by

$$E_s = \frac{0.26}{2} (2000^2 - 1000^2)$$

$$E_s = 3.9 \times 10^5 \text{ ft-lb}$$

This is an awful lot of energy to be lost, but it follows naturally from the experimental data which, if correct, predicts a squirt spike speed of 2000 ft/sec for the 83-pound device.

Volume at Which Maximum Expansion Speed Occurs

The maximum expansion speed for the fluid piston occurs when the pressure of the detonation products inside the piston equals the stagnation pressure of the atmosphere outside the piston. At this time the sum of the forces is equal to zero and the acceleration of the piston is equal to zero. The polytropic relation for Regime II can be used to find the cloud volume at which the expansion speed is a maximum. At that point $P_g = P_{as}$ and we consider this the end of Regime II. The polytropic equation is

$$V_{IIg} = V_{Ig} \left(\frac{P_{Ig}}{P_{IIg}} \right)^{1/n}$$

In this regime the expanding detonation products are approaching perfect gas conditions so that the exponent, n, will be approximately 1.3.

The atmospheric pressure can be calculated from the gas dynamic equation for compressible flow:

$$P_{as} = P_a \left(1 + \frac{K-1}{2} \frac{v^2}{a^2} \right)^{\frac{K}{K-1}} \qquad (9)$$

where

a = sonic speed

K = gas constant

Three-Pound Device

To find the atmospheric stagnation pressure we assume the values

P_a = ambient pressure = 2120 psf

K = 1.4 for air

v = 1300 ft/sec (calculated)

a = 1140 ft/sec

Substitution into the above equation gives

$$P_{as} = 2120 \left[1 + 0.4/2 \left(\frac{1300}{1140}\right)^2\right]^{\frac{1.4}{1.4-1}}$$

$$P_{as} = 4770 \text{ psf}$$

The initial volume of the gaseous detonation products is given by

$$V_{Ig} = V_{Ip} - V_{\ell} = 8.95 \times 10^{-2} - 5.18 \times 10^{-2}$$

$$V_{Ig} = 3.77 \times 10^{-2} \text{ ft}^3$$

and the initial pressure of the detonation products is 1.70×10^5 psf.

Substitution in the polytropic equation results in

$$V_{IIg} = (3.77 \times 10^{-2}) \left(\frac{1.70 \times 10^5}{4.77 \times 10^3}\right)^{1/1.3}$$

$$V_{IIg} = 0.589 \text{ ft}^3$$

The volume of the fluid piston or main body of the cloud[6] is then

$$V_{IIp} = V_{IIg} + 0.9V_{\ell} = 0.589 + 0.047$$

$$V_{IIp} = 0.636 \text{ ft}^3$$

[6]Note that we have accounted for the loss of liquid to the squirt spikes (about 10%) in making this calculation.

The radius of the fluid piston or main body of the cloud at this time is then

$$r_{IIp} = \sqrt{\frac{V_{IIp}}{\pi L}} = \sqrt{\frac{0.636}{\pi \times 0.833}}$$

$$r_{IIp} = 0.49 \text{ ft}$$

Note that the cloud radius at which maximum speed occurs is little more than one canister diameter. This accounts for the fact that any increase of cloud speed is difficult to detect in the experimental data.

Eighty-Three Pound Device

The volume at which maximum expansion speed occurs can be calculated for the eighty-three pound device in a manner similar to that for the three-pound device. If we assume that the maximum cloud speed will be approximately the same as for the three-pound device the dynamic pressure outside the cloud will be 4770 psf. The gas volume at maximum speed will then be

$$V_{IIg} = V_{Ig} \left(\frac{P_{Ig}}{P_{IIg}}\right)^{1/n} = 8.3 \times 10^{-2} \left(\frac{3.6 \times 10^6}{4.77 \times 10^3}\right)^{1/1.3}$$

$$V_{IIg} = 13.7 \text{ ft}^3$$

The piston volume will be

$$V_{IIp} = V_{IIg} + 0.9\, V_L = 13.7 + 0.9\,(1.43)$$

$$V_{IIp} = 15.0 \text{ ft}^3$$

and the main body radius will be

$$r_{IIp} = \sqrt{\frac{V_{IIp}}{\pi L}} = \sqrt{\frac{15.0}{\pi\ 1.6}}$$

$$r_{IIp} = 1.73 \text{ ft}$$

Maximum Cloud Speed in Regime II

The maximum cloud speed can be obtained by substituting the volume at which maximum speed occurs (V_{IIp}) in the equation of motion for Regime II (Eq. 8), and substituting the other appropriate values.

Three-Pound Device

The following value are given:

$V_{\ell} = (5.18 \times 10^{-2})\ 0.9 - 4.66 \times 10^{-2}\ ft^3$

$V_{Ig} = 3.77 \times 10^{-2}\ ft^3$

$V_{Ip} = 8.95 \times 10^{-2}\ ft^3$

$m_{\ell} = 0.093\ (0.9) = 0.084\ slug$

$P_{Ig} = 1.70 \times 10^{5}\ psf$

$v_I^2 = 1.25 \times 10^{6}\ ft^2/sec^2$

$V_{IIg} = 0.589\ ft^3$

$V_{IIp} = 0.636\ ft^3$

$P_{as} = 4770\ psf$

$n = 1.3$

$E_s = 2500\ ft\text{-}lb$

Substituting in Eq. 8 we get

$$v_{II}^2 = \frac{\frac{4.66 \times 10^{-2}}{2}}{0.636} + 0.589 \left\{ \frac{2}{0.084} \left[\frac{(1.70 \times 10^{5})(3.77 \times 10^{-2})^{1.3}}{1 - 1.3} \right.\right.$$

$$\left. (0.589^{-0.3} - 0.0377^{-0.3}) - (4.77 \times 10^{3})(0.636 - 0.0895) - 2500 \right]$$

$$\left. + \frac{(8.95 \times 10^{-2})(1.25 \times 10^{2})}{\frac{4.66 \times 10^{-2}}{2} + 3.77 \times 10^{-2}} \right\}$$

$$v_{II}^2 = 1.92 \times 10^6 \text{ ft}^2/\text{sec}^2$$

$$v_{II} = 1380 \text{ ft/sec}$$

A second iteration would improve the value for the maximum speed if this value were substituted back into Eq. 9 but the improvement would not be significant.

This is the maximum speed of the edge of the cloud for the three pound device in Regime II, and occurs at the end of the regime. From this point, the speed of the cloud decreases.

It is interesting to compare the increase of the average cloud speed from Regime I to Regime II with the increase of the cloud edge speed from Regime I to Regime II. The average cloud speed at the end of Regime I is

$$v_{aI} = v_I \sqrt{\frac{V_{Ip}}{\frac{V_\ell}{2} + V_{Ig}}} = 1100 \sqrt{\frac{8.95 \times 10^{-2}}{\frac{5.18 \times 10^{-2}}{2} + 3.77 \times 10^{-2}}}$$

$$v_{aI} = 1300 \text{ ft/sec}$$

and the average cloud speed at the end of Regime II is

$$v_{aII} = v_{II} \sqrt{\frac{V_{IIp}}{\frac{V_\ell}{2} + V_{IIg}}} = 1380 \sqrt{\frac{0.642}{\frac{4.66 \times 10^{-2}}{2} + 0.589}}$$

$$v_{aII} = 1415 \text{ ft/sec}$$

Note that the edge of the cloud increased some 280 ft/sec in speed whereas the average speed increases only 115 ft/sec as shown by the table below:

	Average Speed	Cloud Edge Speed
Regime I	1300	1100
Regime II	1415	1380

Eighty-Three Pound Device

The maximum cloud speed at the end of Regime II can be calculated in a manner similar to that for the three-pound device by substituting

the appropriate values as follows:

$V_{\ell} = 1.29 \text{ ft}^3$

$V_{Ig} = 8.3 \times 10^{-2} \text{ ft}^3$

$V_{Ip} = 1.51 \text{ ft}^3$

$m_{\ell} = 2.32 \text{ slugs}$

$P_{Ig} = 3.6 \times 10^{6} \text{ psf}$

$v_I^2 = 8.18 \times 10^{5} \text{ ft}^2/\text{sec}^2$

$V_{IIg} = 13.7 \text{ ft}^3$

$V_{IIp} = 15.0 \text{ ft}^3$

$P_{as} = 4770 \text{ psf}$

$n = 1.3$

$E_s = 3.9 \times 10^{5} \text{ ft-lb}$

Substitution in Eq. 8 results in

$$v_{II}^2 = \frac{\frac{1.29}{2} + 13.7}{15.0} \left\{ \frac{2}{2.32} \left[\frac{(3.6 \times 10^6)(8.3 \times 10^{-2})}{1 - 1.3}^{1.3} (13.7^{-0.3} - 0.083^{-0.3}) - (4.47 \times 10^3)(15.0 - 1.51) - 3.9 \times 10^5 \right] + \frac{1.51(8.18 \times 10^5)}{\frac{1.29}{2} + 0.083} \right\}$$

$v_{II}^2 = 1.91 \times 10^{6} \text{ ft}^2/\text{sec}^2$

$v_{II} = 1380 \text{ ft/sec}$

REGIME III

In Regime III the cloud will begin to decelerate since the pressure within the piston is less than the pressure outside the piston. The gas within the piston will continue to expand and its pressure will decrease

until some limiting value of over-expansion is reached as a result of leakage from the outside, at which time the pressure will begin to return to atmospheric. The limiting value of the pressure within the piston is the pressure as expressed by the polytropic relation for any given expansion ratio. This latter pressure could never be reached in an actual situation because the piston is becoming less coherent and is probably breaking up into discrete liquid particles. There will be a leakage of air into the center of the piston from the top, bottom, and through the walls of the fluid piston. This leakage will have two effects:

1. The overexpansion process will be less pronounced since the pressure differential across the piston will be reduced, and

2. The liquid particles will be moving at a relative speed with respect to the air leaking into the center of the piston, which will cause aerodynamic drag. In order to simplify the analysis we are forced to neglect this drag in Regime III.[7]

At the same time the stagnation pressure outside the piston will decrease, although at a lesser rate, because the speed of the expanding piston is decreasing. The minimum value of the stagnation pressure is one atmosphere for zero cloud speed.

During this regime the fragments will begin to pull ahead of the main body of the cloud and to pass the squirt spikes. The fragments are never immersed in the cloud. They are always at the cloud edge for their particular angular position. Some of the droplets of the main body will have moved outward further between the fragments during Regime II and the squirt spikes will have been at greater radius earlier.

It is during this regime that the fragment spikes begin to form. Since the fragments have relatively large surface areas they form wakes behind them. As the fragments move outward with increasing speed relative to the main body of the cloud they entrain some of the droplets in their wakes and carry them outward at speeds greater than the remainder of the cloud.[8] Those droplets form the fragment spikes. The fragments gradually leave the droplets behind, however, and the spikes then decelerate rapidly in the ambient atmosphere.

---

[7]The apparent effect of this simplifying assumption is only speculative, but appears negligible.

[8]The mass loss to the fragment spikes is not accounted for in the remaining analysis since it is essentially negligible in comparison to the total mass for these specific designs.

Equation of Motion

The equation of motion will have the same general form as that for Regime II. The only forces acting on the piston will be the pressure force from the detonation products pressing outward and the stagnation pressure force of the atmosphere outside the piston.

Although the cloud is probably breaking up into discrete droplets we continue to treat the cloud as a fluid piston and ignore the effects of aerodynamic drag on the individual droplets as a result of leakage through the piston. It is impossible to determine how serious an error this introduces, but the complexity of attempting to deal with an equation of motion treating both the fluid mass and the individual droplets in the same equation makes it necessary. The analysis is semi-empirical in this regime because we can't determine the influence of such factors as leakage of air from the outside atmosphere into the inside of the piston.

Regime III is probably the most important phase of the expansion process and yet is the one in which we are least able to predict the results analytically. About 80% of the expansion of the cloud occurs in this regime.

In the case of the three-pound device the experimental data indicates that the relation between the radius of the cloud and the time seems to change at a time of about 5.5 msec (see Fig. 9). From Fig. 12 the same phenomenon seems to take place at a time of about 30 msec in the case of the 83-pound device. This appears to be the point where the fluid piston effect breaks down and some other effect becomes predominant. We will assume that Regime III ends at this point and that another regime with a different equation of motion begins. The apparent dividing line between Regime III and Regime IV occurs at cloud volume of about 55 ft^3 in the case of the three-pound device and a volume of about 2600 ft^3 in the case of the 83-pound device (see Fig. 11 and 13).

The equation of motion for Regime III is obtained from the energy equation

$$P_g dV_g - P_{as} dV_p = m_\ell v dv \qquad (10)$$

Since the pressure outside the piston is the stagnation pressure we rewrite

$$P_{as} = P_a \left(1 + \frac{K-1}{2} \frac{v^2}{a^2}\right)^{K/K-1}$$

The presence of the speed term in the equation for stagnation pressure and also in the kinetic energy relationship makes the equation of motion quite difficult to integrate in that form. It would be possible to resort to numerical techniques to integrate the equation, but since, as will be shown later, an empirical relation is necessary to describe the gas pressure (P_g) versus volume relationship, it did not seem practical

to try to preserve the analytical form of the stagnation pressure equation. It was more practical to resort to an empirical relation for that term also and preserve the capability of integrating the equation of motion.

Based on that reasoning, it was decided to derive an empirical relationship between atmospheric pressure and volume using the experimental data for the three-pound and 83-pound devices to determine the atmospheric pressure-volume relationships.

Furthermore, the shape of the experimental cloud speed versus volume curve (as illustrated by Fig. 13) suggests that the rate of decrease of the speed with respect to the volume must decrease with an increase in volume. Hence, the pressure pushing inward on the piston must become less as expansion proceeds. Because the pressure of the detonation products pushing outward is by definition the same as the stagnation pressure of the atmosphere at the beginning of this Regime, the net force must increase rather than decrease (at least during the first portion of the Regime). It was further assumed that the pressure-volume relationships are as shown schematically in Fig. 17. During the first portion of Regime III (identified as Regime IIIA) the net retarding force increases because the gas pressure inside the piston decreases more rapidly than the stagnation pressure outside the piston decreases. The gas pressure inside the piston drops to atmospheric pressure and then overexpands slightly because of inertia effects before starting to rise back to atmospheric pressure. The atmospheric stagnation pressure, on the other hand, decreases smoothly to some pressure greater than ambient atmospheric pressure at the end of the Regime. The second part of Regime III we call Regime IIIB. The empirical equation of motion will be different for each of these subregimes and each will be treated separately.

We can only assume a value for the terminal gas pressure inside the piston at the end of Regime IIIB since we have no experimental information. A reasonable assumption is one atmosphere since leakage of air through the top and bottom of the piston would tend to equalize the inside and outside pressures. The stagnation pressure outside the piston does have a value greater than one atmosphere, however, since the piston is moving at an appreciable speed and we are assuming negligible leakage through the face of the fluid piston. The amount of overexpansion must also be assumed, mainly on the basis of forcing the cloud speed-volume relationship to have the desired value.

Three-Pound Device

In order to determine an equation of motion for the three-pound device it was first necessary to find an empirical relation between the stagnation pressure of the atmosphere and the volume of the cloud. This was done by using the experimental data of Fig. 11. By the use of the cloud speeds obtained from Fig. 11 it was possible to calculate the stagnation pressure as a function of volume as shown in Fig. 18. The resulting curve was then fitted by an empirical equation of the form

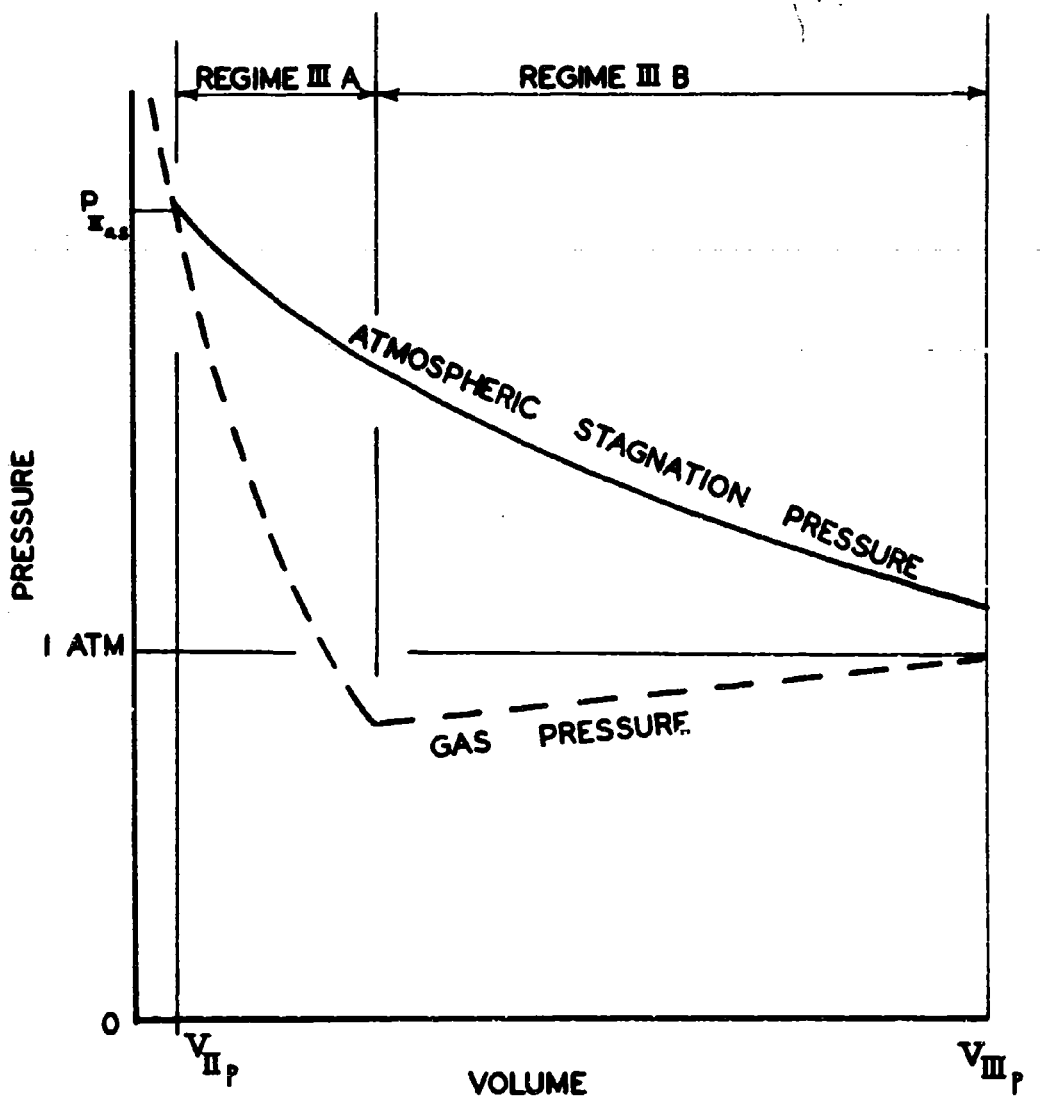

FIG. 17. Schematic of Pressure-Volume Relationships in Regime III.

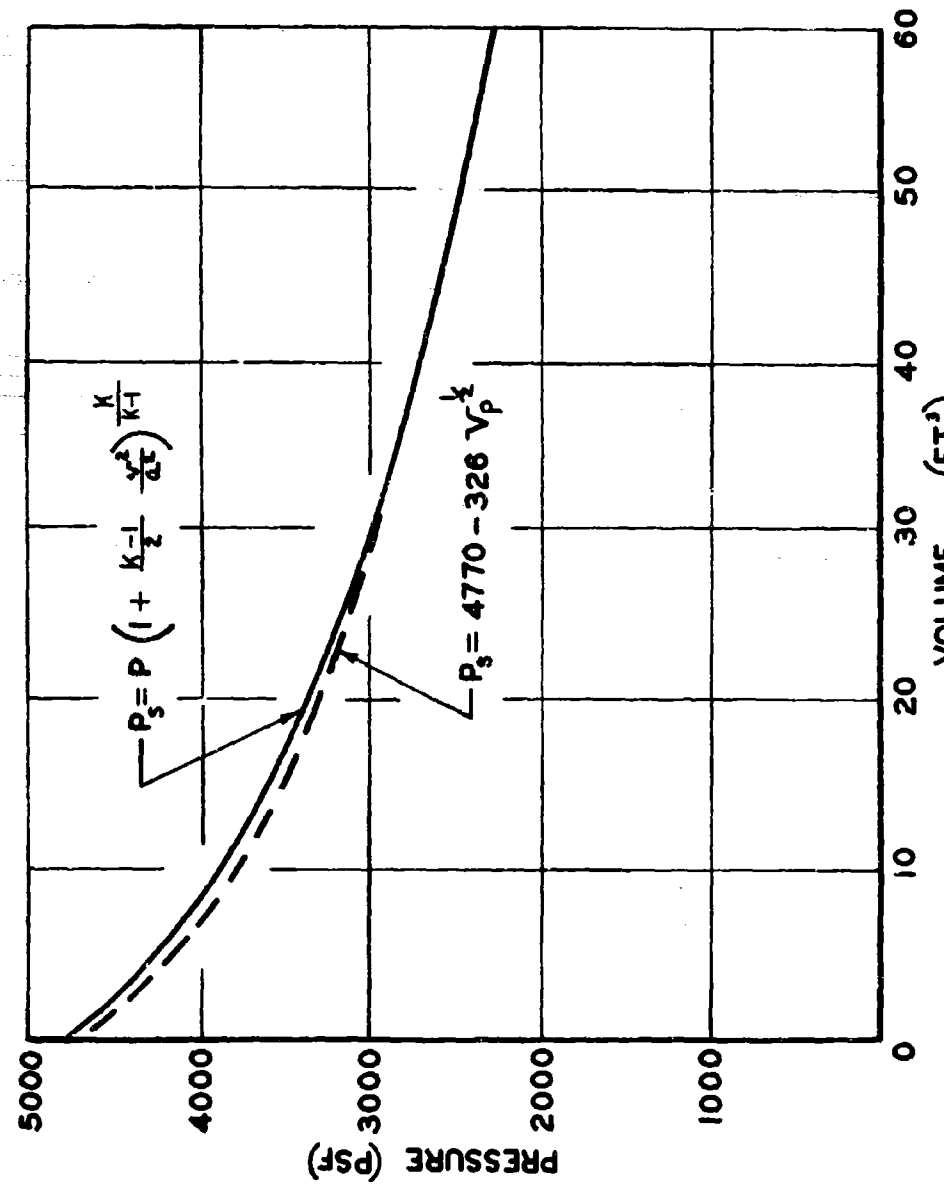

FIG. 18. Dynamic Pressure as a Function of Cloud Volume Three-Pound Device.

$$P = A + BV^{C} \qquad A, B \text{ \& } C \text{ are constant}$$

and the resulting equation, which is a reasonably good fit, is

$$P_{as} = 4770 - 326\, V_p^{1/2} \tag{11}$$

This equation is valid for the entire Regime III for the three-pound device.

Regime IIIA

The relation for the gas pressure inside the piston has different forms for Regimes IIIA and IIIB. For Regime IIIA we use the polytropic relation which is

$$P_g = P_{IIg} \left(\frac{V_{IIg}}{V_g}\right)^n \tag{12}$$

where n is the polytropic exponent if there are no leakage effects. In this case the exponent may be considered a modified polytropic constant which also accounts for the effects of atmospheric leakage into the interior of the piston. The effect of leakage into the interior of the piston is similar to decreasing the value of n since the leakage would tend to lessen the drop in pressure during the expansion process. This was not necessary for our gross calculations, so n = 1.3 was used.

Substitution of Eq. 11 and 12 into Eq. 10 results in

$$\int_{V_{IIg}}^{V_g} P_{IIg} \left(\frac{V_{IIg}}{V_g}\right)^n dV_g - \int_{V_{IIp}}^{V_p} (4770 - 326 V_p^{1/2})\, dV_p = \int_{V_{II}}^{v} m_\ell v\, dv$$

which can be integrated to give the equation of motion for Regime IIIA.

$$v^2 = \frac{2}{m_\ell}\left[\frac{P_{IIg} V_{IIg}^{\,n}}{1-n}\left(V_g^{1-n} - V_{IIg}^{1-n}\right) - 4770\left(V_p - V_{IIp}\right) + 217\left(V_p^{3/2} - V_{IIp}^{3/2}\right)\right]$$

$$+ v_{II}^{2} \tag{13}$$

Substitution of the appropriate numbers gives the numerical form

$$v^2 = 23.8(-7970V_g^{-0.3} - 4770\ V_p + 217\ V_p^{3/2} + 12050) + 1.90 \times 10^6 \quad (14)$$

To find the piston speed at the end of Regime IIIA we select an assumed value for P_g and use the polytropic relation to solve for V_g at the end of Regime IIIA. If we assume that the gas overexpands to 1750 psf

$$V_{IIIAg} = 1.27\ ft^3$$

$$V_{IIIAp} = V_{IIIAg} + V_\ell = 1.32\ ft^3$$

These values can be substituted into Eq. 14 to give

$$v_{IIIA}^2 = 1.88 \times 10^6\ ft^2/sec^2$$

$$v_{IIIA} = 1370\ ft/sec$$

Regime IIIB

In this sub-regime the relation for the atmospheric stagnation pressure remains the same, but the relation for the gas pressure is different. We assume the gas pressure increases from 1750 psf at a volume of 1.32 ft^3 to 2120 psf at 55 ft^3 according to the relation

$$P_g = 1660 + 6.90V_p \quad (15)$$

Substitution of Eq. 15 into the equation of motion gives[9]

$$\int_{V_{IIAp}}^{V_p} (1660 + 6.90\ V_p)\ dV_p - \int_{V_{IIIAp}}^{V_p} (4770 - 326\ V_p^{1/2})\ dV_p$$

$$= \int_{v_{IIIA}}^{v} m_\ell v dv$$

which can be integrated to give the equation of motion for Regime IIIB. Making the appropiate substitutions

[9] We assume that the piston volume equals the gas volume in this sub-regime since their difference becomes negligible as the cloud expands.

$$v^2 = 23.8 \left[+ 3.45\ V_p^{\ 2} + 217\ V_p^{\ 3/2} - 3110\ V_p + 3700\right] + 1.88 \times 10^6 \quad (16)$$

To find the piston speed at the end of Regime IIIB we substitute the piston volume at the end of Regime III which is assumed to be 55 ft^3 and solve for the speed.

$$v^2 = 0.26 \times 10^6\ ft^2/sec^2$$

$$v = 510\ ft/sec$$

Using the same methods we can calculate the speed for volumes from 1.32 ft^3 to 55 ft^3 and plot a curve of speed versus volume. This curve is shown in Fig. 11. It can be seen that the curve compares well with the experimental data.

Eighty-Three-Pound Device

The equation of motion for the 83-pound device is similar to that for the three-pound device. The schematic relations between pressure and volume are shown in Fig. 17, which is valid for the 83-pound device as well as for the three-pound device. In order to develop an equation of motion we take the curve for the main body speed as a function of time and determine an empirical relation between the atmospheric stagnation pressure and volume as we did for the three-pound device. Using the data from Fig. 13 for main body speed the stagnation pressure of the atmosphere ahead of the cloud was calculated by means of Eq. 9. This is plotted in Fig. 19. An empirical equation of the form

$$P_{as} = 13620 - 7140\ V_p^{\ 0.06} \quad (17)$$

was then fitted to the experimental data. As can be seen from Fig. 19, the fit is quite good. Equation 17 is valid for both Regime IIIA and Regime IIIB for the 83-pound device.

Regime IIIA

With the substitution of the polytropic equation for the variation of the gas pressure in Regime IIIA and Eq. 17 the equation of motion becomes

$$\int_{V_{IIg}}^{V_g} P_{IIg} \left(\frac{V_{IIg}}{V}\right)^n dV - \int_{V_{IIp}}^{V_p} (13620 - 7140\ V^{0.06})\ dV = \int_{v_{II}}^{v} m_\ell v dv$$

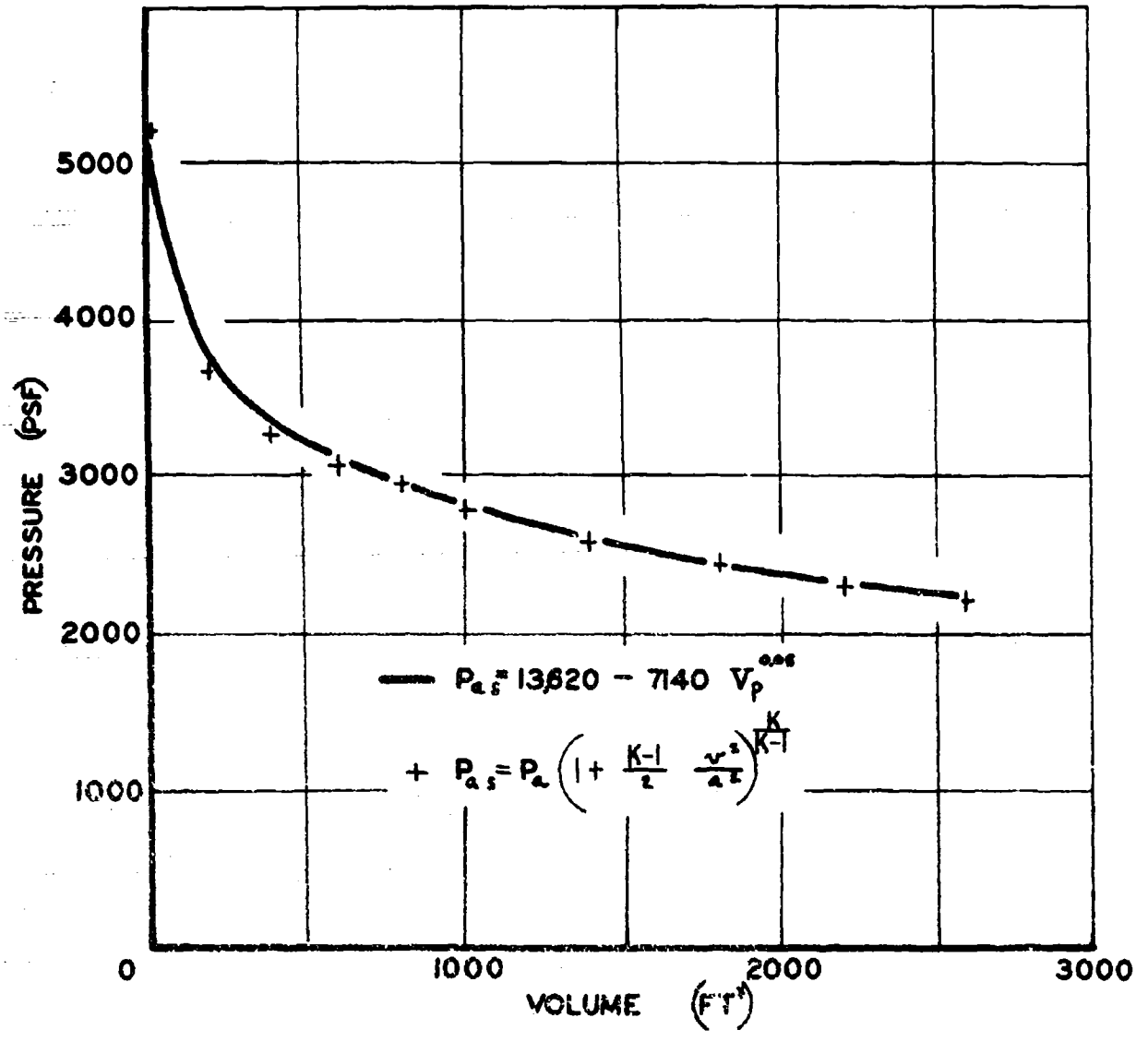

FIG. 19. Dynamic Pressure as a Function of Volume 83 Pound Device.

or

$$v^2 = \frac{2}{m_\ell}\left[\frac{P_{IIg}V_{IIg}^{n}}{1-n}\left(V_g^{1-n} - V_{IIg}^{1-n}\right) - 13620\left(V_p - V_{IIp}\right)\right.$$

$$\left. + 6730\left(V_p^{1.06} - V_{IIp}^{1.06}\right) + v_{II}^2\right] \qquad (18)$$

To find the cloud speed at the end of Regime IIIA we need the values of V_g and V_p at the end of Regime IIIA. If we assume a value of $n = 1.3$ and if we allow the gas to again expand to 1750 psf as for the three-pound device we can calculate V_{IIIAg} by the polytropic equation to get

$$V_{IIIAg} = 31.7 \text{ ft}^3$$

$$V_{IIIAp} = V_{IIIAg} + V_\ell = 31.7 + 1.3 = 33.0 \text{ ft}^3$$

Substitution of the above values into Eq. 18 along with the known values results in

$$v_{IIIA}^2 = \frac{2}{2.32}\left[\frac{5200(13.7)^{1.3}}{1 - 1.3}\left(31.7^{-0.3} - 13.7^{-0.3}\right)\right.$$

$$\left. - 13620\left(33.0 - 15.0\right) + 6730\left(33.0^{1.06} - 15.0^{1.06}\right)\right] + 1.91 \times 10^6$$

$$v_{IIIA}^2 = 1.88 \times 10^6 \text{ ft}^2/\text{sec}^2$$

$$v_{IIIA} = 1370 \text{ ft/sec}$$

Regime IIIB

In Regime IIIB we can use the stagnation pressure relation given by Eq. 17, but a new relation for the gas pressure inside the cloud is required. If we assume that the gas pressure increases from 1750 psf at the end of Regime IIIA to atmospheric pressure (2120 psf) at the end of Regime IIIB the linear gas pressure versus volume relation becomes

$$P = 1740 + 0.144V \qquad (19)$$

This can be substituted along with Eq. 17 into the equation of motion to give

$$\int_{V_{IIIAp}}^{V_p} (1740 - 0.144V)\,dV - \int_{V_{IIIAp}}^{V_p} (13620 - 7140V^{0.06})\,dV = \int_{v_{IIIA}}^{v} m_\ell v\,dv$$

or, upon integration

$$v^2 = \frac{2}{m_\ell} - \Big[11880\,(V_p - V_{IIIAp}) + 0.072\,(V_p^{\,2} - V_{IIIAp}^{\,2}) + 6730\,(V_p^{\,1.06} - V_{IIIAp}^{\,1.06})\Big] + v_{IIIA}^{\,2} \qquad (20)$$

To find the speed at the end of Regime IIIB we substitute the appropriate values for volume and speed to get

$$v_{IIIB}^{\,2} = \frac{2}{2.32} - \Big[11880\,(2600 - 33) - 0.072\,(2600^2 - 33^2) + 6730\,(2600^{1.06} - 33^{1.06})\Big] + 1.88 \times 10^6$$

$$v_{IIIB}^{\,2} = 7.0 \times 10^4 \text{ ft}^2/\text{sec}^2$$

$$v_{IIIB} = 260 \text{ ft/sec}$$

The relationship between speed and volume calculated from Eq. 20 is shown in Fig. 13. It can be seen that the agreement is quite good.

It should be noted that the agreement between actual and calculated values is not so important as the fact that the same equation of motion and the same set of assumptions were used for both the three-pound and the 83-pound analyses and that agreement was reached in both cases. Hence, it seems that the present approach is reacting to the scaling factors correctly.

This empirical approach was used only as a preliminary attempt. It should be possible to insert the gas dynamic equation in the equation of motion and integrate the resulting equation by numerical techniques to eliminate the empirical relation between atmospheric dynamic pressure and cloud volume. Considerable work will be required to determine the actual relations between internal gas pressure of the detonation products and volume, however. At present we have no information concerning the amount of leakage into the interior of the cloud, the amount of overexpansion, and so forth. Until we can get this information there is no way to eliminate the empirical relation between internal gas pressure and volume. The actual relations should be determined.

REGIME IV

In the previous regimes we neglected the effect of aerodynamic drag on the fluid droplets in the main body of the cloud and assumed that the fluid piston was the primary factor influencing the dispersion process. In Regime IV we assume that the fluid piston has disintegrated and that aerodynamic drag on the individual droplets completely controls the dispersion. Neither of these assumptions is correct, of course. Actually both aerodynamic drag and the fluid piston affect the disperson process simultaneously. In order to make the model susceptible to analysis, however, it was necessary to simplify it in this manner. The regime is assumed to begin when the total volume of the cloud with respect to the liquid droplets becomes sufficiently large so that the effects of atmospheric entrainment become negligible and ends when cloud motion for all practical purposes ceases. In the two sizes of devices studied there is a definite breakover point in the radius-time curve which seems to indicate the end of Regime III and the beginning of Regime IV.

In order to simplify the problem we further assume that the pressure of the expanding detonation products is equal to the pressure of the atmosphere, that the atmosphere is motionless, and that the only force acting on the droplet is aerodynamic drag.

Equation of Motion

The equation of motion for the droplet is

$$\Sigma F = F_d = m_d a = - \frac{\rho_a}{2} C_d A_d v_d^2$$

where

m_d = mass of liquid droplet

a = droplet deceleration = $v \frac{dv}{dR}$

v = droplet speed

R = droplet distance from center of cloud

ρ_a = atmospheric density

C_d = droplet drag coefficient

A_d = droplet frontal area

v_d = droplet speed with respect to the atmosphere

Since the Reynolds number is approximately 1000 the above equation should be a good approximation to the actual drag relation.

We can rewrite the equation in the form

$$-\frac{dv_d}{v_d} = \frac{\rho_a C_d A_d}{2\, m_d}\, dR$$

since the atmospheric speed is assumed to be zero. If the atmospheric speed were not zero v would not be the same as v_d.

The ratio of the droplet area to the droplet mass can be written

$$\frac{A_d}{m_d} = \frac{\pi r_d^2}{4/3\pi r_d^3 \rho_d} = \frac{3}{4\rho_d r_d}$$

r_d = droplet radius

ρ_d = droplet density

The equation can be rewritten, therefore, in the form

$$-\frac{dv_d}{v_d} = \frac{0.375\, \rho_a C_d}{\rho_d r_d}\, dR$$

Except for the droplet density, each of the quantities on the right-hand side of the equation is a function of the distance, R. Since the atmospheric density, the drag coefficient(6), and the droplet radius all decrease with time or Reynolds number, we can assume, as a first approximation, that their quotient is constant. Therefore we can write:

$$\frac{0.375\, \rho_a C_d}{\rho_d r_d} = \text{const.} = K$$

Thus

$$-\frac{dv}{v} = K\,dR$$

$$-\int_{v_{IIId}}^{v_d} \frac{dv}{v} = K \int_{R_{III}}^{R} dR$$

Upon integration we get

$$- \ell n_e v_d + \ell n_e v_{IIId} = K (R - R_{III})$$

In order to make the above equation compatible with the equation of motion for the other three regimes we use

$$R = \sqrt{\frac{V}{\pi L}}$$

and the equation becomes

$$\ell n_e v_d = \ell n_e v_{IIId} - \sqrt{\frac{K^2}{\pi L}} \left(V^{1/2} - V_{III}^{1/2}\right)$$

or

$$v_d = \exp \left[\ell n_e v_{IIId} - \sqrt{\frac{K^2}{\pi L}} \left(V^{1/2} - V_{III}^{1/2}\right)\right] \qquad (21)$$

This is the equation of motion for a single cloud droplet in Regime IV. By substituting appropriate values for the variables we can make it applicable to either the three-pound or 83-pound device.

Three-Pound Device

The constant K is

$$K = \frac{\rho_a C_d A_d}{2 m_d} = 0.375 \frac{\rho_a C_d}{\rho_d r_d}$$

We can substitute representative values as follows:

$\rho_a = 0.0024$ slug/ft^3

$C_d = 0.80$

$\rho_d = 1.80$ slug/ft^3

$r_d = 0.0002$ ft

The droplet radius is representative of values which have been obtained by Stanford Research Institute in their studies (Ref. 2) whereas the drag coefficient is representative of the drag coefficient to be expected of a spherical droplet in this Reynolds number regime. The constant, K, therefore becomes

$$K = \frac{0.375(0.0024)(0.80)}{(1.80)(0.0002)} = 2.00$$

Upon substitution of the following values

$$L = 0.834 \text{ ft}$$

$$v_{IIId} = 510 \text{ ft/sec}$$

$$V_{III} = 55 \text{ ft}^3$$

the equation of motion becomes

$$v_d = \exp\left[6.2 - 1.24\,(V^{1/2} - 7.42)\right] \qquad (22)$$

By the use of Eq. 22 we can solve for the droplet speed for various values of V. For instance, when V equals 80 ft^3 the speed is given by

$$v_d = \exp\left[6.2 - 1.24\,(8.94 - 7.42)\right] = 75 \text{ ft/sec}$$

Fig. 11 shows the calculated speed versus cloud volume curve for Regime IV. Agreement with the experimental data is good.

Maximum Cloud Radius

The maximum cloud radius can be obtained by allowing the droplet speed to decay to a negligible value and then solving for the volume. For instance, if we assume that the maximum radius is reached when v = 5 ft/sec or

$$v_{II} = 0.01\, v_{III}$$

We can solve for the maximum volume, V_{IV},

$$V_{IV}^{1/2} = V_{III}^{1/2} + \frac{\ell n_e \dfrac{v_{IIId}}{v_{IVd}}}{\sqrt{\dfrac{K^2}{\pi L}}}$$

$$= \frac{\ell n_e 100}{1.24} + 55^{1/2}$$

$$V_{IV} = 124 \text{ ft}^3$$

The maximum cloud radius is then

$$R_{IV} = \sqrt{\frac{V_{IV}}{\pi L}} = \sqrt{\frac{124}{\pi\ (0.83)}}$$

$$R_{IV} = 6.9 \text{ ft}$$

This value agrees fairly well with the available experimental data as shown in Fig. 10.

Eighty-Three Pound Device

The constant, K, becomes

$$K = 0.33$$

when the following representative values are substituted:

$$V_{IIId} = 260 \text{ ft/sec}$$

$$V_{IIId} = 2600 \text{ ft}^3$$

$$L = 1.60 \text{ ft}$$

$$\rho_a = 0.0024 \text{ slugs/ft}^3$$

$$\rho_d = 1.80 \text{ slugs/ft}^3$$

$$C_d = 0.40$$

$$r_d = 0.0006 \text{ ft}$$

The larger droplet size with its resultant lower drag coefficient can be justified on the basis of the lower burster charge to liquid ratio of the 83-pound device as compared to the three-pound device. The lower energy per unit mass of liquid resulting from the lower burster charge to liquid ratio would tend to result in larger droplets. Experimental evidence has confirmed that the larger device produces larger droplets.

The equation of motion, therefore, becomes

$$v_d = \exp\left[5.56 - 0.147\ (V^{1/2} - 51)\right] \qquad (23)$$

for the 83-pound device. Figure 13 illustrates the cloud speed calculated by the use of Eq. 23 compared to the cloud speed taken from experimental data.

Maximum Cloud Radius

If we allow the droplet size to decay to the same value as for the three-pound device (5 ft/sec) then

$$v_{dIV} = 0.02 v_{dIII}$$

and the equation becomes

$$V_{IV}^{1/2} = \frac{\ell n_e \, 50}{0.147} + 51$$

$$V_{IV} = 5930 \text{ ft}^3$$

The maximum cloud radius is then given by

$$R_{IV} = \sqrt{\frac{5930}{1.6\,\pi}}$$

$$R_{IV} = 33 \text{ ft}$$

This value is somewhat greater than the experimental value given by Fig. 12, but is within 10% at a time of 0.10 seconds.

SUMMARY

The equations of motion which have been developed in this report match the experimental data which is available for two sizes of explosive dispersion devices. Those devices represent the largest and smallest devices for which we have experimental information, and hence the equations seem to be reacting correctly to the scaling requirements.

The equations are based on the concept of a fluid piston in the first three regimes of motion. This fluid piston is essentially a gas bubble surrounded by a liquid shell. As the gas bubble expands it forces the liquid outward to form the characteristic explosive dispersion cloud.

In Regime I, in which the canister expands before rupturing, the maximum cloud speed (which is the same as the expansion speed of the metal canister), is calculated to be 1100 ft/sec for the three-pound canister. This is almost exactly the same as the initial speed of the fragments from the three-pound canister as measured experimentally. No data is available concerning the speed of the fragments from the 83-pound device, but the calculated value of 904 ft/sec is reasonable in

view of the lower burster charge-to-liquid ratio of the larger device and the fact that the initial elongation of the steel canister for the larger device appears to be less than that for the aluminum canister for the smaller device. Since the canister walls are accelerating in this regime the sooner they rupture the lower their maximum speed will be. It would be helpful to get some experimental information on the true time of rupture of the steel canister of the 83-pound device to verify this assumption. It might also be helpful to compare the time of rupture for both aluminum and steel canisters for devices of the same size.

As a result of the earlier rupture of the steel canister the pressure inside the canister at the end of Regime I will be greater for the 83-pound device than for the three-pound device. This greater pressure would account for the much greater initial cloud speed which was measured for the 83-pound device. Since the only portion of the cloud which can be measured very early in the expansion is the squirt jet, the experimentally determined initial cloud speed of about 2000 ft/sec for the 83-pound device must be the squirt jet speed. This is much greater than the 1340 ft/sec measured for the three-pound device and would require an internal pressure of some 25,000 psi.

In Regime II the liquid cloud is still accelerating because the pressure inside the canister is greater than the pressure outside the canister. The maximum cloud speed is reached when the pressures inside and outside are equalized. That is the end of Regime II. The equation of motion predicts that the maximum cloud speed for the three-pound device will be 1380 ft/sec and that it occurs at a cloud radius of about 0.5 ft. The maximum speed for the 83-pound device is also about 1380 ft/sec and occurs at a cloud radius of about 1.8 ft. These speeds and distances are compatible with the experimental information. Note that the radius at which the maximum speed occurs is quite small as calculated from the equation of motion. Analysis of the experimental information reveals that it is very difficult to detect an increase in speed of the cloud initially because it occurs so close to the point of detonation. Only on very high-speed cameras, such as the Cordin camera, can the initial acceleration of the cloud be detected.

In Regime III the cloud begins to decelerate. This regime is the one in which most of the cloud expansion occurs, but it is the one which we are least able to handle analytically because so little information on the actual processes within the cloud is available. By assuming semi-empirical relations based upon what knowledge we have of the physics of the cloud expansion we were, however, able to develop an equation of motion which gave reasonable results for both the small three-pound canister and the large 83-pound canister.

We need considerably more information on the expansion dynamics, including overexpansion, leakage, and the individual droplet effects, before we can replace the empirical relationships with theoretical relationships. We think, however, that once this information is available, the basic equation of motion will be satisfactory. The speed-distance relationships obtained from the equation of motion match those obtained from experiment quite closely. It should be realized, however, that even the experimental speed-distance relationships are only approximations. It is quite difficult to get reliable speed-distance values by graphical differentiation of the available radius-time information.

The speed at the end of Regime III was calculated to be 510 ft/sec for the three-pound device and 260 ft/sec for the 83-pound device. While these are values quite close to those which would be expected, the nature of the equation is such that very small variations in the numerical values assumed for the equation result in large variations in the final calculated cloud speeds. We aren't, for example, justified in assuming that the actual droplet speed for the three-pound device is greater than that for the 83-pound device at the end of this regime based upon the calculations. The uncertainty is such that the speeds could well be reversed. Hence, the final speeds indicate only that the equations of motion are able to produce reasonable relationships between speed and distance when reasonable numerical values are used in the equations.

In Regime IV we shift our analysis to look at the individual droplets. We abandon the fluid piston concept and concentrate on aerodynamic drag of the droplets as the controlling factor. In the analysis we assume that the fluid piston disintegrates instantaneously at the end of Regime III and aerodynamic drag of the droplets takes over immediately as the controlling factor. This is not really the case. Aerodynamic drag on the droplets is probably influencing the expansion before the fluid piston disintegrates completely. The assumption does seem to reflect the existence of a breakover point in the experimental radius-time curves at which the drag seems to increase markedly. The droplets at that point seem to slow down almost instantaneously, as if the aerodynamic drag were suddenly becoming predominant. This sudden decrease is shown in the experimental data of Fig. 11 and 13 and is reflected in the calculated values for the equations of motion. This seems to indicate that the actual transition from the fluid piston effect to the aerodynamic drag effect might be quite abrupt in reality as well as in theory.

The measured diameter of the cloud at maximum expansion is less than that predicted by the equation of motion in the case of the 83-pound device and greater than that predicted by the equation for the three-pound device. A major reason for the difference is the use of a droplet speed of 260 ft/sec at the beginning of the regime for the 83-pound device and a speed of 510 ft/sec for the three-pound device as calculated from Regime III, and the interdependence of the drag coefficient and the droplet radius.

What is important, is that in both cases the values obtained are reasonably close to the experimental values. Whenever assumptions were made they were based on physical evidence or reasonable extrapolations from physical evidence. It was not necessary to introduce any unfounded "fudge factors" in order to make the equations of motion balance for both the three-pound and 83-pound devices, and multiple iterations would improve the agreement with experimentally observed motion.

CONCLUSIONS

The major conclusion which we have drawn from this study is the importance of the fluid piston in determining the size to which the explosively dispersed cloud will expand. It appears that the cloud expands to some critical size as a result of the piston effect at which point the piston effect deteriorates rapidly and the expansion rate of the cloud rapidly approaches zero.

This critical size is directly related to the size of the device, and we believe that it is a direct function of the thickness of the liquid column surrounding the gaseous detonation products. When this liquid shell becomes too thin to effectively prevent the leakage of air in large quantities through the piston into its interior, the drag of the atmospheric air rushing past the droplets from the outside of the piston to the inside because of the pressure gradient between the inside and outside becomes the dominating factor and the droplets slow down almost immediately.

If this is the case, then the factor dominating the size of the expanding cloud will be the initial thickness of the liquid column surrounding the burster charge, which is effectively the diameter of the explosive dispersion device. The greater the diameter of the device the greater will be the ultimate size of the cloud.

A certain amount of burster explosive will be required to disperse the liquid, but the device does not seem to be highly sensitive to the burster charge-to-liquid ratio. The three-pound device had twice the burster explosive for every pound of liquid compared to the 83-pound device, but the cloud diameter of the smaller device was obviously not twice the size of that for the larger device. The most obvious effects of the higher burster charge-to-liquid ratio will be to slightly increase the speed of the expansion and to break the liquid into smaller droplets. Smaller droplets might delay the decay of the piston by providing a less permeable shell, but, on the other hand, they will slow down more rapidly in the aerodynamic regime of flight.

Another effect of the larger burster charge ratio will be to force more liquid into the squirt spikes. Since the material in the squirt spikes might be wasted material, any factor which takes liquid out of the main body and forces it into the squirt spikes might be undesirable.

The influence of the canister material also appears to be secondary. The steel canister appears to rupture earlier than the aluminum canister, forcing more material into the squirt spikes. The energy required to burst the canister in either case, however, is much less than that available to accelerate the liquid in the main body so that the effect of the canister material on the dispersion of the main body of the cloud is slight in terms of expansion distance. Effort should be devoted toward developing a material which will minimize the amount of liquid in both the squirt spikes and the fragment spikes. A canister material which would rupture into minute fragments, thus eliminating the squirt spikes and the fragment spikes, and which would also provide additional material to reinforce the shell of the fluid piston, might well improve the performance of the device.

Since the overexpansion of the gases within the interior of the piston strongly influences the expansion of the piston by creating a negative pressure gradient it might be possible to increase the expansion distance by allowing leakage into the interior of the piston from the top and bottom during the latter stages of the expansion. This would eliminate the adverse pressure gradient so that the negative expansion work would be less, and would also decrease the tendency of the atmospheric air to force its way into the piston through the liquid shell, thus prolonging Regime III of the expansion process.

In order to increase the size of the expanding cloud in the aerodynamic regime of flight two possibilities present themselves. The first of these is the use of a more dense liquid and the second is the use of a more viscous material. Both of these would increase the travel of the droplets in the aerodynamic regime, although the increase would not be dramatic.

REFERENCES

1. Stanford Research Institute. Explosive Dispersion of Volatile Liquids, by R. C. Robbins. Menlo Park, California, Project PAU-4047 Technical Report No. 8, 22 January 1964. CONFIDENTIAL.

2. U. S. Naval Ordnance Test Station, Inyokern. Fuel-Air Explosive Clouds, Part 2, Explosive Dispersion of Volatile Liquids, by R. C. Robbins. China Lake, Calif., NOTS, October 1965. (NavWeps Report 8660, Part 2), CONFIDENTIAL.

3. U. S. Naval Ordnance Test Station, Inyokern. Exploratory Development Problems in FAX Weaponization, Transactions of the Fourth Symposium on Warhead Research, by Richard J. Zabelka, Douglas G. Kinney, and Lloyd H. Smith. China Lake, Calif., NOTS, 1965. (TP 3984), CONFIDENTIAL.

4. Cook, M. A., The Science of High Explosives, Reinhold, New York, 1958, p. 284.

5. Reinhard, John S. and John Pearson, Behavior of Metals Under Impulsive Loads, Dover, New York, 1965, pp. 16-17.

6. Schlichting, Hermann, Boundary Layer Theory, Fourth Ed., McGraw-Hill, New York, 1960, p. 16.

UNCLASSIFIED
Security Classification

DOCUMENT CONTROL DATA - R & D

(Security classification of title, body of abstract and indexing annotation must be entered when the overall report is classified)

1 ORIGINATING ACTIVITY (Corporate author) Naval Weapons Center China Lake, California 93555	2a. REPORT SECURITY CLASSIFICATION UNCLASSIFIED 2b. GROUP

3 REPORT TITLE

EXPLOSIVELY DISPERSED LIQUIDS. PART 1, DISPERSION MODEL

4 DESCRIPTIVE NOTES (Type of report and inclusive dates)

5 AUTHOR(S) (First name, middle initial, last name)

Richard J. Zabelka and Lloyd H. Smith

6 REPORT DATE	7a. TOTAL NO OF PAGES	7b. NO OF REFS
December 1969	68	6

8a. CONTRACT OR GRANT NO	9a. ORIGINATOR'S REPORT NUMBER(S)
b. PROJECT NO AirTask A35-532-050/216-1/W11-62X c. d.	NWC TP 4702, Part 1 9b. OTHER REPORT NO(S) (Any other numbers that may be assigned this report)

10 DISTRIBUTION STATEMENT

THIS DOCUMENT IS SUBJECT TO SPECIAL EXPORT CONTROLS AND EACH TRANSMITTAL TO FOREIGN GOVERNMENTS OR FOREIGN NATIONALS MAY BE MADE ONLY WITH PRIOR APPROVAL OF THE NAVAL WEAPONS CENTER.

11 SUPPLEMENTARY NOTES	12 SPONSORING MILITARY ACTIVITY
	Naval Air Systems Command Washington, D. C. 20360

13 ABSTRACT

A preliminary analysis of the dispersion process of liquid droplets into an aerosol cloud is presented. This assessment of the complex phenomena is not all encompassing, but is believed to shed some light upon the behavior of the various mechanisms which govern the expansion of explosively dispersed liquids. This analysis does provide a basic understanding, and provides data for preliminary design estimates.

The equations presented are based on the concept of a fluid piston in the first three of four regimes of motion. This fluid piston is essentially a gas bubble surrounded by a liquid shell. As the gas bubble expands it forces the liquid outward to form the characteristic explosive dispersion cloud. The fluid piston degenerates into discrete droplets, whose motion is governed by aerodynamic forces in Regime IV.

These equations of motion were developed from experimental data collected with two different size devices. The agreement with this data indicates that scaling requirements are satisfied.

DD FORM 1 NOV 65 1473 (PAGE 1)

S/N 0101-807-6801

UNCLASSIFIED
Security Classification

14. KEY WORDS	LINK A		LINK B		LINK C	
	ROLE	WT	ROLE	WT	ROLE	WT
Explosive Dispersion Liquid Cloud Dispersion Model						

ABSTRACT CARD

Naval Weapons Center
Explosively Dispersed Liquids. Part 1, Dispersion Model (U), by Richard J. Zabelka and Lloyd H. Smith. China Lake, Calif., NWC, December 1969. 68 pp. (NWC TP 4702, Part 1), UNCLASSIFIED.

ABSTRACT. A preliminary analysis of the dispersion process of liquid droplets into an aerosol cloud is presented. This assessment of the complex phenomena is not all encompassing, but is believed to shed some light upon the behavior of the various mechanisms which govern the expansion of explosively dispersed liquids. This analysis does provide a basic understanding, and provides data for preliminary design

(Over)
2 cards, 8 copies

Naval Weapons Center
Explosively Dispersed Liquids. Part 1, Dispersion Model (U), by Richard J. Zabelka and Lloyd H. Smith. China Lake, Calif., NWC, December 1969. 68 pp. (NWC TP 4702, Part 1), UNCLASSIFIED.
ABSTRACT. A preliminary analysis of the dispersion process of liquid droplets into an aerosol cloud is presented. This assessment of the complex phenomena is not all encompassing, but is believed to shed some light upon the behavior of the various mechanisms which govern the expansion of explosively dispersed liquids. This analysis does provide a basic understanding, and provides data for preliminary design
(Over)
2 cards, 8 copies

Naval Weapons Center
Explosively Dispersed Liquids. Part 1, Dispersion Model (U), by Richard J. Zabelka and Lloyd H. Smith. China Lake, Calif., NWC, December 1969. 68 pp. (NWC TP 4702, Part 1), UNCLASSIFIED.
ABSTRACT. A preliminary analysis of the dispersion process of liquid droplets into an aerosol cloud is presented. This assessment of the complex phenomena is not all encompassing, but is believed to shed some light upon the behavior of the various mechanisms which govern the expansion of explosively dispersed liquids. This analysis does provide a basic understanding, and provides data for preliminary design
(Over)
2 cards, 8 copies

Naval Weapons Center
Explosively Dispersed Liquids. Part 1, Dispersion Model (U), by Richard J. Zabelka and Lloyd H. Smith. China Lake, Calif., NWC, December 1969. 68 pp. (NWC TP 4702, Part 1), UNCLASSIFIED
ABSTRACT. A preliminary analysis of the dispersion process of liquid droplets into an aerosol cloud is presented. This assessment of the complex phenomena is not all encompassing, but is believed to shed some light upon the behavior of the various mechanisms which govern the expansion of explosively dispersed liquids. This analysis does provide a basic understanding, and provides data for preliminary design
(Over)
2 cards, 8 copies

estimates.

The equations presented are based on the concept of a fluid piston in the first three of four regimes of motion. This fluid piston is essentially a gas bubble surrounded by a liquid shell. As the gas bubble expands it forces the liquid outward to form the characteristic explosive dispersion cloud. The fluid piston degenerates into discrete droplets, whose motion is governed by aerodynamic forces in Regime IV.

(Contd. on Card 2)

NWC TP 4702, Part 1

estimates.

The equations presented are based on the concept of a fluid piston in the first three of four regimes of motion. This fluid piston is essentially a gas bubble surrounded by a liquid shell. As the gas bubble expands it forces the liquid outward to form the characteristic explosive dispersion cloud. The fluid piston degenerates into discrete droplets, whose motion is governed by aerodynamic forces in Regime IV.

(Contd. on Card 2)

NWC TP 4702, Part 1

estimates.

The equations presented are based on the concept of a fluid piston in the first three of four regimes of motion. This fluid piston is essentially a gas bubble surrounded by a liquid shell. As the gas bubble expands it forces the liquid outward to form the characteristic explosive dispersion cloud. The fluid piston degenerates into discrete droplets, whose motion is governed by aerodynamic forces in Regime IV.

(Contd. on Card 2)

NWC TP 4702, Part 1

estimates.

The equations presented are based on the concept of a fluid piston in the first three of four regimes of motion. This fluid piston is essentially a gas bubble surrounded by a liquid shell. As the gas bubble expands it forces the liquid outward to form the characteristic explosive dispersion cloud. The fluid piston degenerates into discrete droplets, whose motion is governed by aerodynamic forces in Regime IV.

(Contd. on Card 2)

ABSTRACT CARD

Naval Weapons Center
Explosively Dispersed Liquids.....(Card 2)
These equations of motion were developed from experimental data collected with two different size devices. The agreement with this data indicates that scaling requirements are satisfied.

NWC TP 4702, Part 1

Naval Weapons Center
Explosively Dispersed Liquids.....(Card 2)
These equations of motion were developed from experimental data collected with two different size devices. The agreement with this data indicates that scaling requirements are satisfied.

NWC TP 4702, Part 1

Naval Weapons Center
Explosively Dispersed Liquids.....(Card 2)
These equations of motion were developed from experimental data collected with two different size devices. The agreement with this data indicates that scaling requirements are satisfied.

NWC TP 4702, Part 1

Naval Weapons Center
Explosively Dispersed Liquids.....(Card 2)
These equations of motion were developed from experimental data collected with two different size devices. The agreement with this data indicates that scaling requirements are satisfied.

NWC TP 4702, Part 1

ABSTRACT CARD

Naval Weapons Center
Explosively Dispersed Liquids. Part 1, Dispersion Model (U), by Richard J. Zabelka and Lloyd H. Smith. China Lake, Calif., NWC, December 1969. 68 pp. (NWC TP 4702, Part 1), UNCLASSIFIED.

ABSTRACT. A preliminary analysis of the dispersion process of liquid droplets into an aerosol cloud is presented. This assessment of the complex phenomena is not all encompassing, but is believed to shed some light upon the behavior of the various mechanisms which govern the expansion of explosively dispersed liquids. This analysis does provide a basic understanding, and provides data for preliminary design

(Over)

2 cards, 8 copies

Naval Weapons Center
Explosively Dispersed Liquids. Part 1, Dispersion Model (U), by Richard J. Zabelka and Lloyd H. Smith. China Lake, Calif., NWC, December 1969. 68 pp. (NWC TP 4702, Part 1), UNCLASSIFIED.

ABSTRACT. A preliminary analysis of the dispersion process of liquid droplets into an aerosol cloud is presented. This assessment of the complex phenomena is not all encompassing, but is believed to shed some light upon the behavior of the various mechanisms which govern the expansion of explosively dispersed liquids. This analysis does provide a basic understanding, and provides data for preliminary design

(Over)

2 cards, 8 copies

Naval Weapons Center
Explosively Dispersed Liquids. Part 1. Dispersion Model (U), by Richard J. Zabelka and Lloyd H. Smith. China Lake, Calif., NWC, December 1969. 68 pp. (NWC TP 4702, Part 1), UNCLASSIFIED.

ABSTRACT. A preliminary analysis of the dispersion process of liquid droplets into an aerosol cloud is presented. This assessment of the complex phenomena is not all encompassing, but is believed to shed some light upon the behavior of the various mechanisms which govern the expansion of explosively dispersed liquids. This analysis does provide a basic understanding, and provides data for preliminary design

(Over)

2 cards, 8 copies

Naval Weapons Center
Explosively Dispersed Liquids. Part 1. Dispersion Model (U), by Richard J. Zabelka and Lloyd H. Smith. China Lake, Calif., NWC, December 1969. 68 pp. (NWC TP 4702, Part 1), UNCLASSIFIED

ABSTRACT. A preliminary analysis of the dispersion process of liquid droplets into an aerosol cloud is presented. This assessment of the complex phenomena is not all encompassing, but is believed to shed some light upon the behavior of the various mechanisms which govern the expansion of explosively dispersed liquids. This analysis does provide a basic understanding, and provides data for preliminary design

(Over)

2 cards, 8 copies

NWC TP 4702, Part 1

estimates.

The equations presented are based on the concept of a fluid piston in the first three of four regimes of motion. This fluid piston is essentially a gas bubble surrounded by a liquid shell. As the gas bubble expands it forces the liquid outward to form the characteristic explosive dispersion cloud. The fluid piston degenerates into discrete droplets, whose motion is governed by aerodynamic forces in Regime IV.

(Contd. on Card 2)

NWC TP 4702, Part 1

estimates.

The equations presented are based on the concept of a fluid piston in the first three of four regimes of motion. This fluid piston is essentially a gas bubble surrounded by a liquid shell. As the gas bubble expands it forces the liquid outward to form the characteristic explosive dispersion cloud. The fluid piston degenerates into discrete droplets, whose motion is governed by aerodynamic forces in Regime IV.

(Contd. on Card 2)

NWC TP 4702, Part 1

estimates.

The equations presented are based on the concept of a fluid piston in the first three of four regimes of motion. This fluid piston is essentially a gas bubble surrounded by a liquid shell. As the gas bubble expands it forces the liquid outward to form the characteristic explosive dispersion cloud. The fluid piston degenerates into discrete droplets, whose motion is governed by aerodynamic forces in Regime IV.

(Contd. on Card 2)

NWC TP 4702, Part 1

estimates.

The equations presented are based on the concept of a fluid piston in the first three of four regimes of motion. This fluid piston is essentially a gas bubble surrounded by a liquid shell. As the gas bubble expands it forces the liquid outward to form the characteristic explosive dispersion cloud. The fluid piston degenerates into discrete droplets, whose motion is governed by aerodynamic forces in Regime IV.

(Contd. on Card 2)

ABSTRACT CARD

Naval Weapons Center
Explosively Dispersed Liquids.....(Card 2)
These equations of motion were developed from experimental data collected with two different size devices. The agreement with this data indicates that scaling requirements are satisfied.

NWC TP 4702, Part 1

Naval Weapons Center
Explosively Dispersed Liquids.....(Card 2)
These equations of motion were developed from experimental data collected with two different size devices. The agreement with this data indicates that scaling requirements are satisfied.

NWC TP 4702, Part 1

Naval Weapons Center
Explosively Dispersed Liquids.....(Card 2)
These equations of motion were developed from experimental data collected with two different size devices. The agreement with this data indicates that scaling requirements are satisfied.

NWC TP 4702, Part 1

Naval Weapons Center
Explosively Dispersed Liquids.....(Card 2)
These equations of motion were developed from experimental data collected with two different size devices. The agreement with this data indicates that scaling requirements are satisfied.

NWC TP 4702, Part 1